The New Cornwall syenogranite, Nova Scotia: petrology and geochemistry

G. Pe-Piper and S. Ingram

Department of Geology, Saint Mary's University, Halifax, NS B3H 3C3

<gpiper@stmarys.ca>

The New Cornwall syenogranite is a 1.7 km^2 intrusion at the southern margin of the Whale Lake monzogranite of the South Mountain Batholith of southwestern Nova Scotia. It has a mean SiO_2 content of 75.8%, and contains accessory amounts of tourmaline, andalusite, and primary muscovite. Ratios such as A/CNK (~ 1.25), Rb/K (~ 215), and Nb/Ta (~ 3.5) show that the syenogranite is not highly fractionated. Although binary element plots for some elements show the same regular trend for both monzogranite and syenogranite, variations in trace elements such as Rb, Ba, Th and LREE show that the syenogranite is not derived from the monzogranite by fractional crystallization, as the syenogranite has lower Eu and HREE compared with the monzogranite. Similarities in LREE, Nd isotope composition (ε_{Nd} ~ -2) and other geochemical indicators between monzogranite and syenogranite suggest that they were derived by partial melting of a common source. Both the Whale Lake monzogranite and the New Cornwall syenogranite then evolved independently by fractional crystallization and late fluids played only a minor role in the further evolution of the syenogranite. This represents a third mode of development of mineralized leucogranite in the South Mountain Batholith, in addition to the previously recognized "associated" and "independent" leucogranite.

Le syénogranite de New Cornwall constitue une intrusion de 1,7 kilomètre carré sur la limite méridionale du granite monzonitique du lac Whale, lequel fait partie du batholithe du mont South, dans le sud-ouest de la Nouvelle-Écosse. Il a une teneur moyenne en SiO_2 de 75,8 %, et renferme des quantités accessoires de tourmaline, d'andalousite et de muscovite primaire. Les rapports d'A/CNK (~ 1,25), de Rb/K (~ 215) et de Nb/Ta (~ 3,5) révèlent que le syénogranite n'est pas extrêmement fractionné. Même si les représentations graphiques des éléments binaires de certains éléments révèlent la même tendance régulière dans le cas du granite monzonitique et du syénogranite, les variations des éléments traces comme le Rb, le Ba, le Th et les éléments de terres rares légers signalent que le syénogranite ne provient pas du granite monzonitique par cristallisation fractionnaire, car le syénogranite possède des teneurs moindres en Eu et en éléments de terres rares lourds comparativement au granite monzonitique. Les similarités existantes en ce qui concerne les éléments de terres rares légers, la composition en isotopes de Nd (ε_{Nd} ~ -2) et d'autres indicateurs géochimiques entre le granite monzonitique et le syénogranite permettent de supposer qu'ils proviennent d'une fonte partielle d'une source commune. Le granite monzonitique du lac Whale et le syénogranite de New Cornwall ont ensuite tous deux évolué indépendamment par cristallisation fractionnaire et les fluides tardifs ont seulement joué un rôle secondaire dans l'évolution ultérieure du syénogranite. Il s'agit là d'un troisième mode de développement du leucogranite minéralisé dans le batholithe du mont South, qui s'ajoute aux leucogranites « associés » et « indépendants » déjà reconnus.

INTRODUCTION

The Devonian South Mountain Batholith (SMB) of southern Nova Scotia (Fig. 1) is a composite plutonic suite of principally granodiorite and monzogranite in the Meguma terrane of the northeastern Appalachian orogen. Siliceous rocks, variously termed leucogranite, leucomonzogranite or syenogranite, form kilometre-scale intrusive bodies that were emplaced mostly late in the evolution of the batholith. Using the definition of Streckeisen (1976), "leuco" applies to igneous rocks with <6% ferromagnesian minerals. In the SMB, MacDonald *et al.* (1992) distinguished leucogranite with <2% biotite from leucomonzogranite with 2–7% biotite.

The New Cornwall syenogranite is a leucogranite in the sense of Streckeisen (1976), although not in the terminology of MacDonald *et al.* (1992) and Horne (1992), and is the only syenogranite body in the SMB. It has an area of about 1.7 km^2, outcrops at the southern part of the Whale Lake monzogranite

unit (Horne 1992) and intrudes, with an exposed intrusive contact, the Goldenville Formation of the Meguma Group at the southern margin of the SMB, on the north side of Caribou Lake (Fig. 1). It contains Mo, Cu, and Bi mineral occurrences (Horne 1992).

The purpose of this study is to better understand the origin of this unique syenogranite through a detailed mineralogical and geochemical study, and to compare this syenogranite with leucogranite and leucomonzogranite elsewhere in the SMB.

PREVIOUS WORK

MacDonald *et al.* (1992) mapped the SMB and described the petrography, geochemistry, and age. They recognized 13 component plutons, grouped into early biotite-bearing monzogranite and granodiorite and later muscovite ± biotite monzogranite – leucomonzogranite – leucogranite. The New
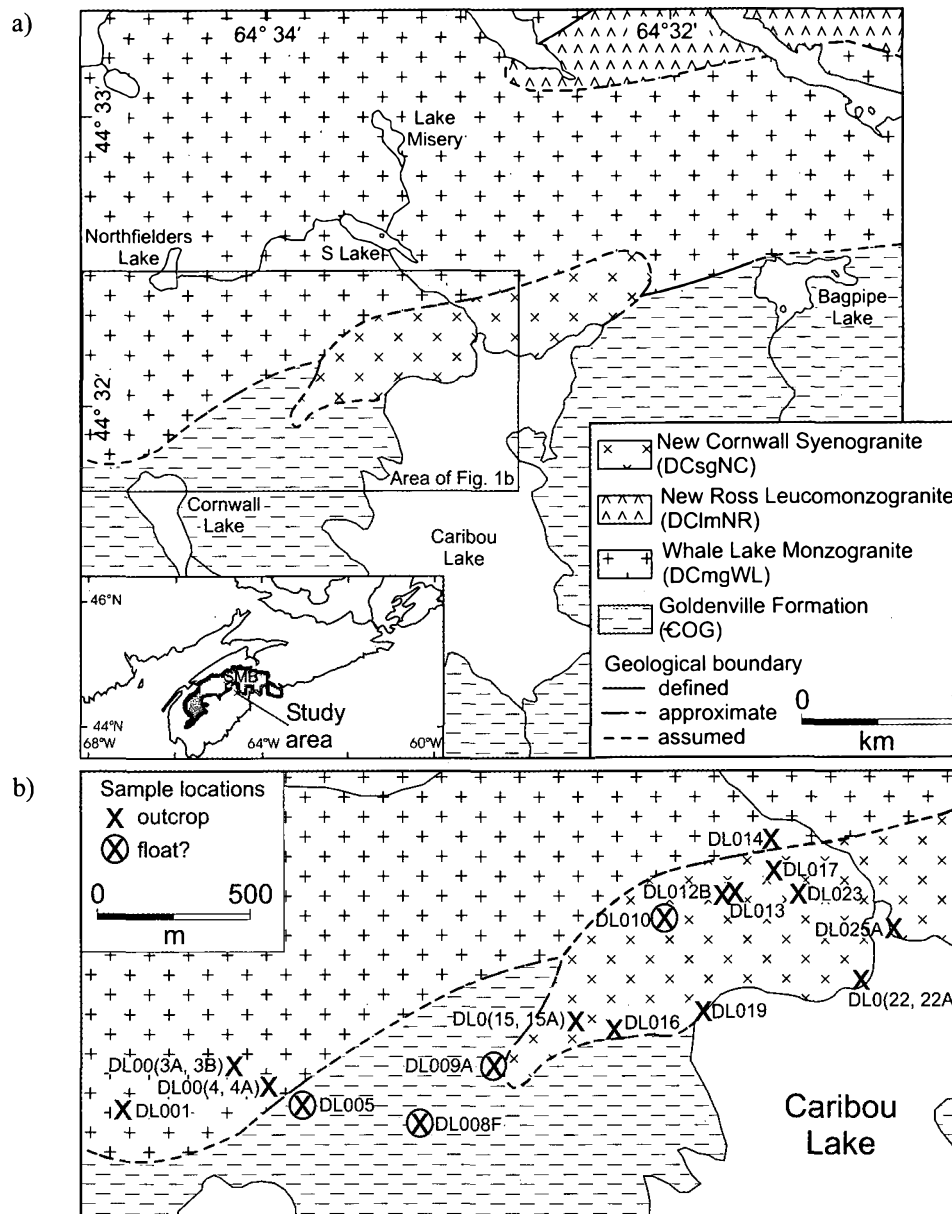
Fig. 1. Geological map (after Horne 1992) showing a) location of the New Cornwall syenogranite and b) the sampled locations. Rock unit codes follow Horne (1992). SMB on inset location map = South Mountain Batholith.

Cornwall syenogranite and Whale Lake monzogranite form part of the New Ross late-stage pluton. The various plutons were generated by melting of protoliths with differing compositions (Smith 1979).

The petrography of the New Cornwall syenogranite and its mineralization are given in Horne (1987, 1992). MacDonald et al. (1992) included the syenogranite in their fine-grained leucomonzogranite, which makes up 6.8% of the batholith. Clarke et al. (1993) presented a comprehensive review and classification of leucogranite bodies within the SMB and classified leucogranite into two categories, "associated" and "independent". The "associated" leucogranite bodies form zones generally <100 m^2, exhibit gradational contacts with fine-grained leucomonzogranite, and were developed by open-system interaction between fluid and leucomonzogranite. The "independent" leucogranite bodies

occur as larger discrete bodies with sharp contacts with other rocks of the batholith and represent highly fractionated melts. Although the volume of leucogranite in the SMB is small (0.7% according to MacDonald et al. 1992), it is host to many of the mineral deposits.

FIELD OBSERVATIONS

We re-examined both the New Cornwall syenogranite and the Whale Lake monzogranite in the field. Horne (1992) mapped the contact as sharp but approximate. We were unable to locate a sharp intrusive contact between the monzogranite and the syenogranite. A contact zone less than 2 m wide was observed on a highly weathered glaciated pavement, but there is no evidence of sharp or dyked contacts on this surface. However, in a loose block of monzogranite, we found a 10 cm
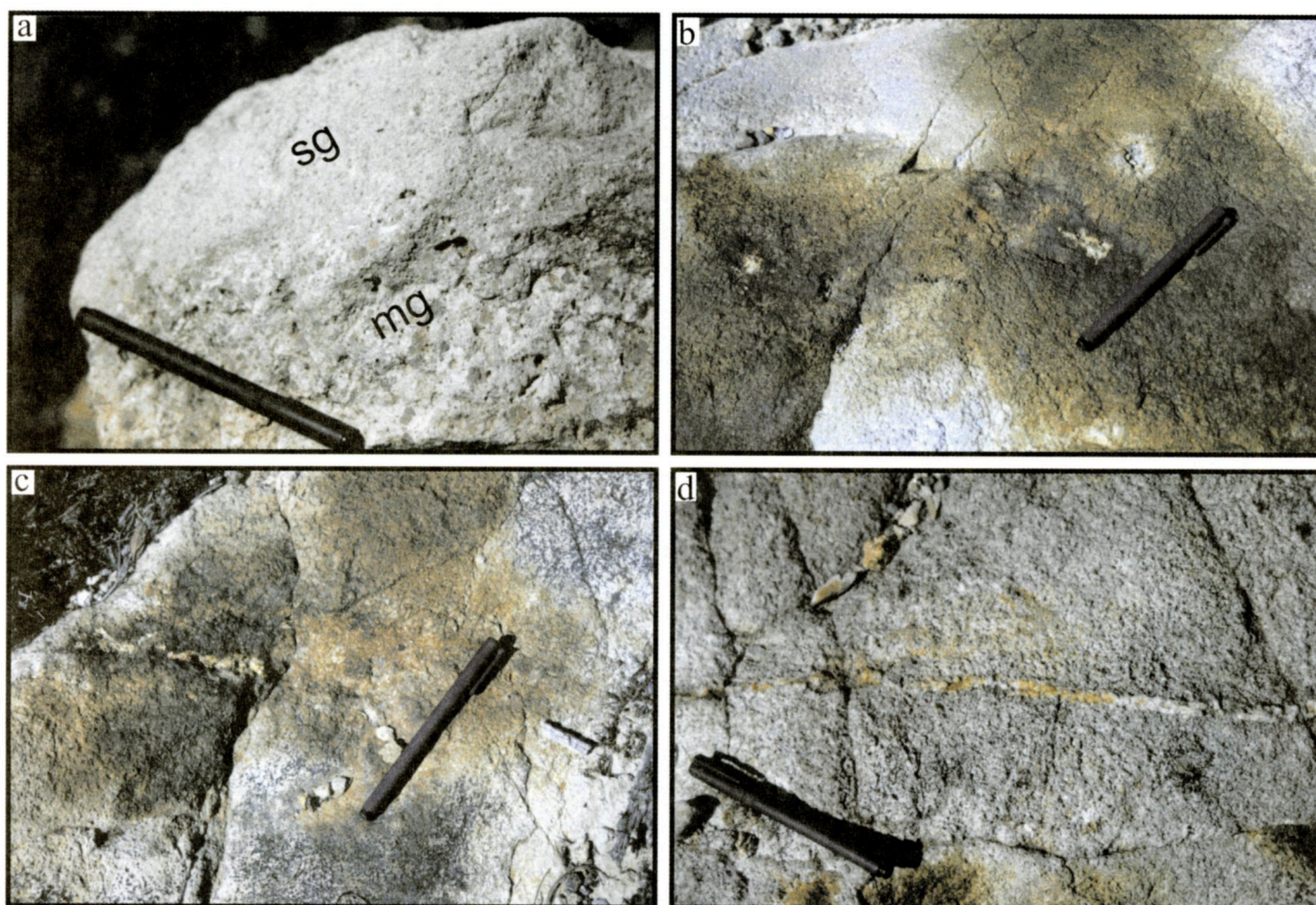
Fig. 2. Outcrop photographs: (a) a loose block of monzogranite with a 10 cm wide dyke of syenogranite. Brown-weathered sulphides and/or other minerals in mineralized syenogranite occurring in (b) miarolitic cavities, (c) along fractures, and (d) in quartz veinlets.

wide dyke of syenogranite (Fig. 2a), thus indicating that the syenogranite intruded the Whale Lake monzogranite.

The New Cornwall syenogranite is a medium-grained rock with rare (<0.1%) miarolitic cavities (Fig. 2b) and pegmatitic mineral clots (Fig. 3b), cut by a few late quartz veins. We disagree with Horne (1987, 1992) who characterized these cavities as being "abundant", making up 1% of the rock. Such cavities occur only locally. The syenogranite contains sulphide mineralization in places, generally following high porosity zones. Mineralization is visible as brown weathered patches in miarolitic cavities (Fig. 2b), along fractures (Fig. 2c), and in quartz veinlets (Fig. 2d). Locally, the syenogranite shows dispersed brown spots (Fig. 3a), presumed to be weathered sulphides, as well as brown halos surrounding miarolitic cavities (Fig. 3c). Aplite is also present within the syenogranite body. Sharp contacts between the syenogranite and the aplite have not been observed, suggesting that the contact between the syenogranite and aplite may be gradational over a short distance. No mafic enclaves or xenoliths of Meguma Group country rock were observed in the syenogranite.

PETROGRAPHY

Whale Lake monzogranite

The Whale Lake monzogranite near Caribou Lake is medium- to coarse-grained, and grey on fresh surfaces. Some samples have large euhedral crystals of plagioclase up to 3 cm in length. However, the majority of the crystals are subhedral and up to 5 mm in diameter. The major minerals include quartz, plagioclase, K-feldspar, and biotite, with accessory amounts of muscovite, chlorite, garnet, tourmaline, zircon, rutile, and apatite (Table 1). In the samples we have studied neither cordierite nor andalusite were observed, although Horne (1987) noted trace amounts of cordierite throughout the Whale Lake monzogranite with up to 1–2% in select zones. The opaque minerals include ilmenite, hematite, rutile, pyrite, chalcopyrite, arsenopyrite, and pyrrhotite (Fig. 4).

The monzogranite is locally altered, with prominent alteration of biotite to chlorite and sericitization of feldspars. Some interstitial muscovite appears to represent alteration of unknown minerals. The most intensely altered parts of the monzogranite weather to yellow and/or orange. A few samples
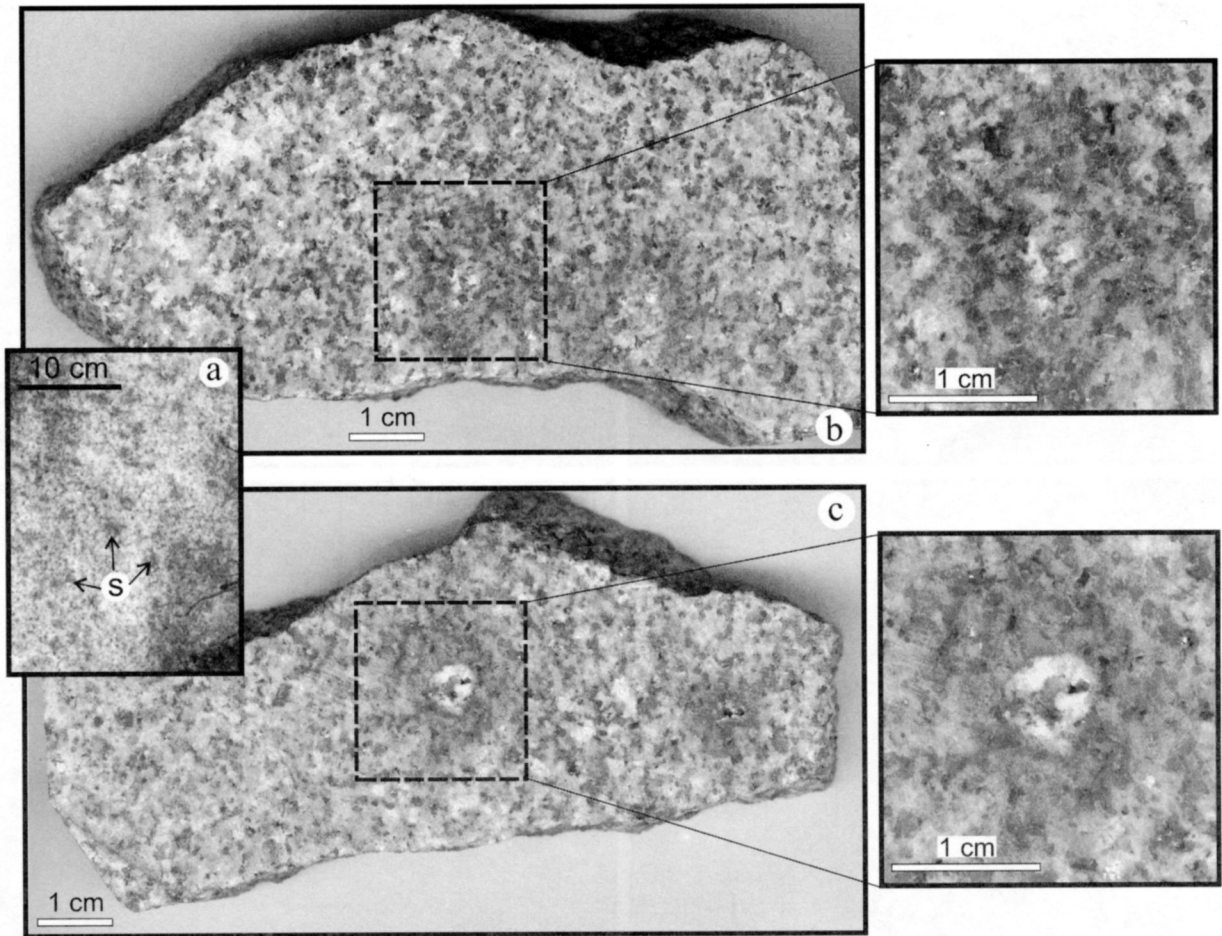
Fig. 3. Mineral clots and miarolitic cavities in the New Cornwall syenogranite. (a) Field photograph with dark (brown) spots (s) some of which occur as halos around miarolitic cavities or mineral clots (DL040). (b) Mineral clot mainly of white feldspar and quartz surrounded by a dark (brown) halo (DL012). (c) Miarolitic cavity partly filled with feldspar and quartz and surrounded by a dark (brown) halo (DL012).
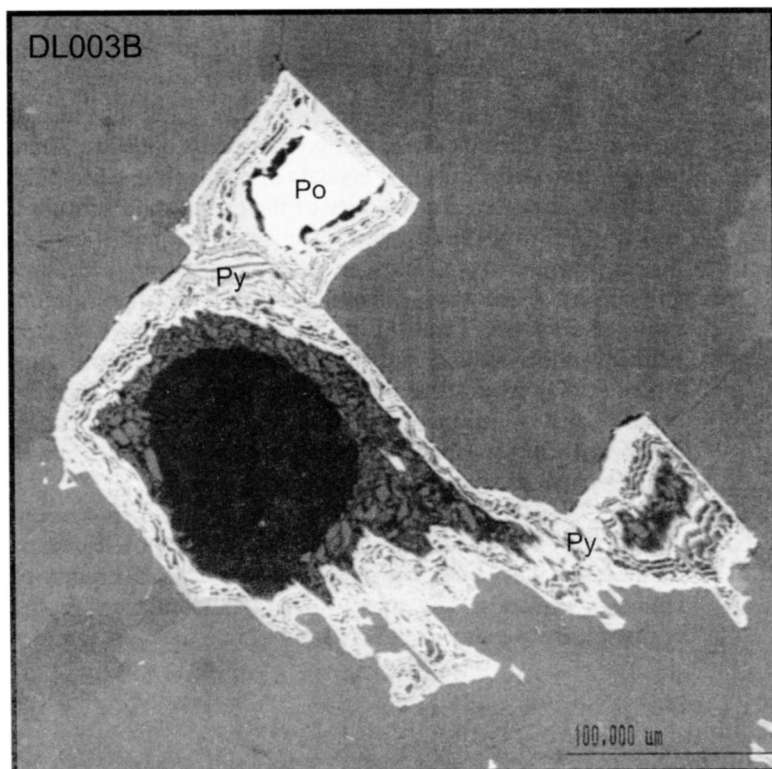

Fig. 4. A back-scattered electron image of pyrite crystal (Py) enclosing pyrrhotite (Po) in a monzogranite (DL003B). The pyrite has weathered away (grey area) leaving a cavity.

Table 1. Petrography of analysed samples

Sample No.	Unit[3]	texture	major minerals	accessory minerals (<5%)	opaque minerals	cavities	alteration / weathering
DL001	DCmg	inequigranular coarse	Qtz, Pl, Kfs, Bt	Ms, Chl, Zrn, Rt, ?Tur, Ap	Ilm, Hem, Py, Apy	small cavities[1]	surface[2] and in cracks
DL003A	DCmg	inequigranular coarse	Qtz, Pl, Kfs, Bt	Chl, Ms, Zrn, Grt, ?Tur	Ilm, Hem, Ccp, Py	small cavities[1]	some spherical patches (not well defined)
DL003B	DCmg	inequigranular coarse	Qtz, Pl, Kfs, Bt	Chl, Zrn, Grt, ?Tur, Ap, Ms	Ilm, Hem, Ccp, Py, Po	small cavities[1]	surface[2]
DL004	DCmg	inequigranular coarse	Qtz, Pl, Kfs, Bt	Chl, Ms, Zrn, Grt, Rt, ?Tur	Ilm, Hem, Ccp	small cavities[1]	pervasive and in veins and fractures
DL004A	DCmg	inequigranular medium	Qtz, Pl, Kfs, Bt	Chl, Ms, Zrn, Grt, Rt, Ap	Ilm, Hem, Ccp, Py	absent	surface[2]
DL005	DCmg	inequigranular coarse	Qtz, Pl, Kfs, Bt	Chl, Ms, Zrn, Ap	Ilm, Hem, Py	absent	pervasive alteration
DL008F	DCmg	inequigranular fine-medium	Qtz, Pl, Kfs, Bt	Chl, Ms, Zrn, Grt, Rt	Ilm, Hem, Py	absent	absent
DL009A	DCmg	inequigranular coarse	Qtz, Pl, Kfs, Bt	Chl, Ms, Zrn, Grt, Rt, Ap	Hem, Ccp, Py	absent	absent
DL010	DCmg	inequigranular medium	Qtz, Pl, Kfs, Bt	Chl, Ms, Zrn, Grt, Ap	Ilm, Hem	absent	surface[2]
DL012B	DCsg	equigranular medium	Qtz, Pl, Kfs, Bt, Chl	Ms, Zrn, Tur	Ilm, Hem, Ccp, Py	miarolitic	well defined alteration halos around cavities
DL013	DCsg	equigranular medium	Qtz, Pl, Kfs, Chl	Bt, Ms, Zrn, Tur	Ilm, Hem	miarolitic	well defined alteration halos around cavities
DL014	DCmg	inequigranular medium	Qtz, Pl, Kfs, Bt	Chl, Ms, Zrn, Rt, Tur, Ap	Ilm, Hem	absent	absent
DL015	DCsg	equigranular fine-medium	Qtz, Pl, Kfs	Chl, Ms, Bt, Zrn, Tur, And	Ilm, Hem, Py	small cavities[1]	surface[2] and pervasivive
DL015A	DCsg	equigranular fine-medium	Qtz, Pl, Kfs	Bt, Ms, Zrn, Crd, Pin, Tur, And	Ilm, Hem, Ccp, Py	small cavities[1]	pervasive
DL016	DCsg	equigranular fine-medium	Qtz, Pl, Kfs, Ms	Bt, Zrn, And	Ilm, Hem, Ccp, Py	miarolitic with crystal growth	surface[2] and in some areas pervasive
DL017	DCsg	equigranular medium	Qtz, Pl, Kfs, Chl	Bt, Zrn, Ms, Rt, Tur	Ilm, Hem	absent	surface[2]
DL019	DCsg	equigranular medium	Qtz, Pl, Kfs, Chl	Bt, Ms, Zrn, Tur, Rt	Ilm, Hem, Py	small cavities[1]	pervasive and alteration halos around cavties
DL022	DCsg	inequigranular fine-medium	Qtz, Pl, Kfs, Bt	Chl, Ms, Zrn, And	Ilm, Hem, Ccp, Py	small cavities[1]	surface[2]
DL022A	DCsg (aplite)	equigranular fine	Qtz, Pl, Kfs, Ms	Chl, Zrn, Tur, And	Ilm, Hem	small miarolitic	surface[2] and in some areas pervasive
DL023	DCsg	equigranular medium	Qtz, Pl, Kfs, Chl	Bt, Ms, Zrn, Tur, Rt	Ilm, Hem	absent	small spherical patches around pyrite crystals
DL025A	DCsg (aplite)	equigranular fine	Qtz, Pl, Kfs	Chl, Ms, Zrn, Tur	Ilm, Hem	absent	pervasive

Mineral abbreviations: And = magmatic andalusite; Ap = apatite; Apy = arsenopyrite; Bt = biotite; Ccp = chalcopyrite; Chl = chlorite; Crd = cordierite; Grt = garnet; Hem = hematite; Ilm = ilmenite; Kfs = K-feldspar; Ms = muscovite; Pin = pinite; Pl = plagioclase; Pn = pentlandite; Py = pyrite; Po = pyrrhotite; Qtz = quartz; Rt = rutile; Tur = Tourmaline; Zrn = zircon

Notes: [1]Small cavities lined with a brown alteration product (cavities are probably the result of complete weathering of pyrite crystals). [2]Surface weathering occurs as a yellowish orange rim on the outer portion of the samples. This rim ranges from < 1 to 3 cm thick. [3]DCmg = Whale Lake monzogranite, DCsg = New Cornwall syenogranite.

contain small (about 1 mm in diameter) cavities. All such cavities have very fine grained brownish yellow alteration material as lining and are probably not miarolitic, but represent a void left by the weathering of pyrite, as seen in Fig. 4.

Modal muscovite ranges from 1.4–3.7% (2.7% on average), based on point counting of thin sections. Primary muscovite is distinguished using the petrographic criteria of Ham and Kontak (1988) and makes up 0.9% of the mode, on average. Modal percentages of biotite range from 6.9–18.2%, with an average of 10.1%. Dark minerals (biotite, chlorite, opaque minerals) average 13.6% and ferromagnesian minerals (biotite, muscovite, chlorite, garnet) represent 14.7%, on average. The plagioclase crystals present have a composition of $An_{2-35}Ab_{64-94}Or_{0-2}$ (average $An_{16}Ab_{83}Or_1$) and the K-feldspar a composition of $An_{0-10}Ab_{2-11}Or_{88-95}$ (average $An_{0.6}Ab_9Or_{91}$).

New Cornwall syenogranite

The New Cornwall syenogranite is in general a medium- to fine-grained rock and light grey on fresh surfaces. Most samples are equigranular and crystals are mainly anhedral to subhedral and average 1–2 mm in diameter. Major minerals are quartz, plagioclase, and K-feldspar, with > 5% biotite, muscovite, and chlorite in some samples. Accessory minerals include zircon, tourmaline, magmatic andalusite, cordierite, and muscovite, with biotite also present in some samples. Ilmenite, hematite, chalcopyrite, pyrite, and minor rutile make up the opaque minerals (Table 1).

Biotite is altered to chlorite. Chlorite of uncertain origin also occurs interstitially through the samples. Yellow and/or orange staining (probably alteration to limonite) occurs pervasively (Fig. 3a), or as outer rims, or as halos around mineral clots (Fig. 3b) or cavities. Well defined halos, about 1 cm in diameter, surround miarolitic cavities (Fig. 3c).

Three types of cavities occur in the syenogranite:
1. Cavities that are lined with brown, weathered crystal relicts. These cavities, up to 4 mm in diameter, are assumed to be left by an opaque mineral, probably pyrite, that has weathered out, similar to what is observed in the monzogranite.
2. Miarolitic cavities that contain well-formed feldspar and quartz crystals. The crystals radiate inwards toward the empty space and may be white or stained yellow. These cavities can have a diameter of up to 7 mm (Fig. 3c) with brown halos up to 1 cm in width. In the mineralized samples (Fig. 2b), these cavities also contain pyrite (very common), and chalcopyrite (common). We looked extensively, using both microscope and electron microprobe, for molybdenite, which is known to occur in leucogranite, but we did not locate it with certainty or in any quantity.
3. There are also abundant pegmatitic "clots" or "pods" of minerals throughout some of the syenogranite samples (Fig. 3b). These mineral clots are white, while the rest of the rock is pink and grey. Minerals in the pods display albitization and silicification. The clots are up to 1 cm in diameter and are mainly spherical or ovoid with an orange alteration halo about 5 mm wide.

Aplite found in the syenogranite has similar mineralogy to the syenogranite except that it lacks biotite. The texture is fine grained, with crystals typically <1 mm and phenocrysts are absent. Some aplite samples contain miarolitic cavities <1 mm in diameter, some of which are lined by minute crystals, but none are surrounded by brown halos.

Modal muscovite content of syenogranite samples ranges from 2.5–6.9% with an average of 4.3%. Primary muscovite is recognized petrographically as single subhedral crystals with sharp outlines that do not appear to be pseudomorphs after andalusite. Such primary muscovite makes up about 1.1% of the mode on average, in similar abundance to that in the monzogranite. Secondary muscovite is more abundant in the syenogranite. Excluding aplite samples, which lack biotite, modal fresh biotite in the syenogranite ranges from 2.4–6.7% with an average of 4.1%. (Partially chloritized biotite was counted, but chlorite lacking any evidence of biotite was not included.) Dark minerals (biotite, chlorite, and opaque minerals) average 8.7% and ferromagnesian minerals (biotite, muscovite, chlorite, andalusite, cordierite) average 11.6%. The range of the plagioclase composition present in the syenogranite is $An_{0.6-29}Ab_{69-99}Or_{0-4}$ (ave. $An_{10}Ab_{88}Or_{1.5}$) and the range of K-feldspar composition is $An_0Ab_{5-19}Or_{81-95}$ (ave. $An_0Ab_{11}Or_{89}$). A plot of modal muscovite vs. modal biotite (Fig. 5) shows that the syenogranite falls either in the overlap zone of the fields for "independent" and "associated" leucogranite bodies, or in the field of coarse-grained leucomonzogranite in the terminology of Clarke et al. (1993). The modal amount of muscovite is consistent with the amounts of muscovite in the "independent" leucogranite, but the amount of primary muscovite is more similar to the "associated" leucogranite group.

WHOLE-ROCK GEOCHEMISTRY

The whole-rock chemistry of 21 representative samples was determined by X-ray fluorescence (major and trace elements) and by instrumental neutron activation analysis (REE and additional trace elements) on selected samples (Table 2). Analytical methods are described by Pe-Piper and Piper (1989).

In the nomenclature of de la Roche et al. (1980) (Fig. 6), almost all the rocks identified petrographically as monzogranite plot in the monzogranite field and all syenogranite samples and one aplite plot in the syenogranite field. The second aplite plots close to the boundary between the syenogranite and alkali granite fields. In the nomenclature of Streckeisen and Le Maitre (1979) (not shown here), the Whale Lake monzogranite samples classify as "syenogranite" and the New Cornwall syenogranite as "alkali-feldspar granite". Both monzogranite and syenogranite plot within the subalkaline field of Irvine and Baragar (1971) (not shown).

Scatter in potentially mobile elements, as is shown in plots of K_2O (Fig. 7g) or Rb (Fig. 8b) vs. SiO_2, appears no greater than in more stable elements such as TiO_2 (Fig. 7b), Y or Zr (Fig. 8e). Many elements show linear trends with little scatter (e.g. Al_2O_3 vs. SiO_2 in Fig. 7a; Rb vs. Ba in Fig. 9d) or tight clusters (e.g. Sr vs. SiO_2 in Fig. 8c). This suggests that
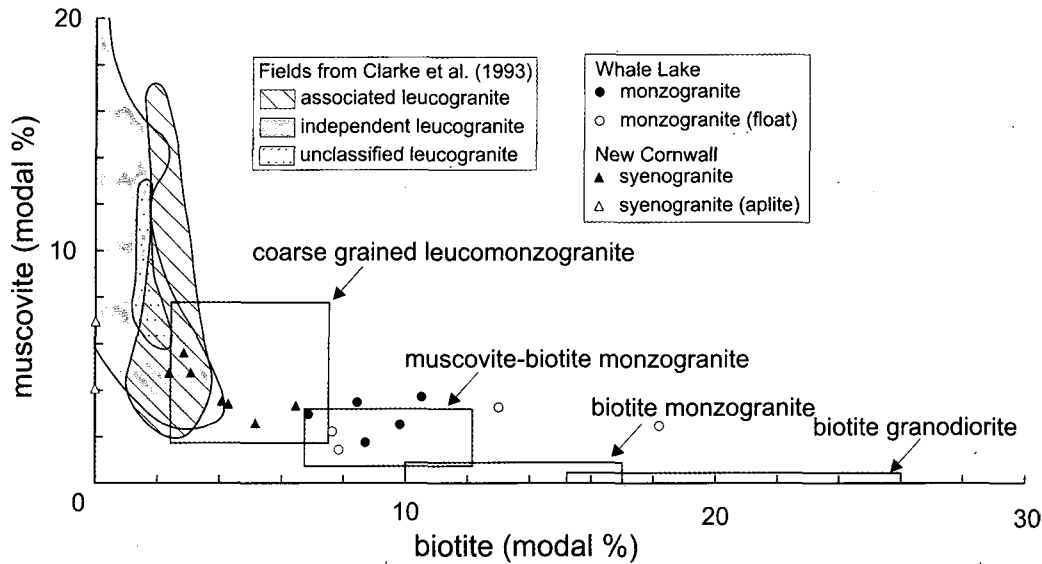
Fig. 5. Modal percentages of biotite and muscovite in the various granitoid types of the SMB (after Clarke *et al.* 1993) compared with modal compositions from this study.
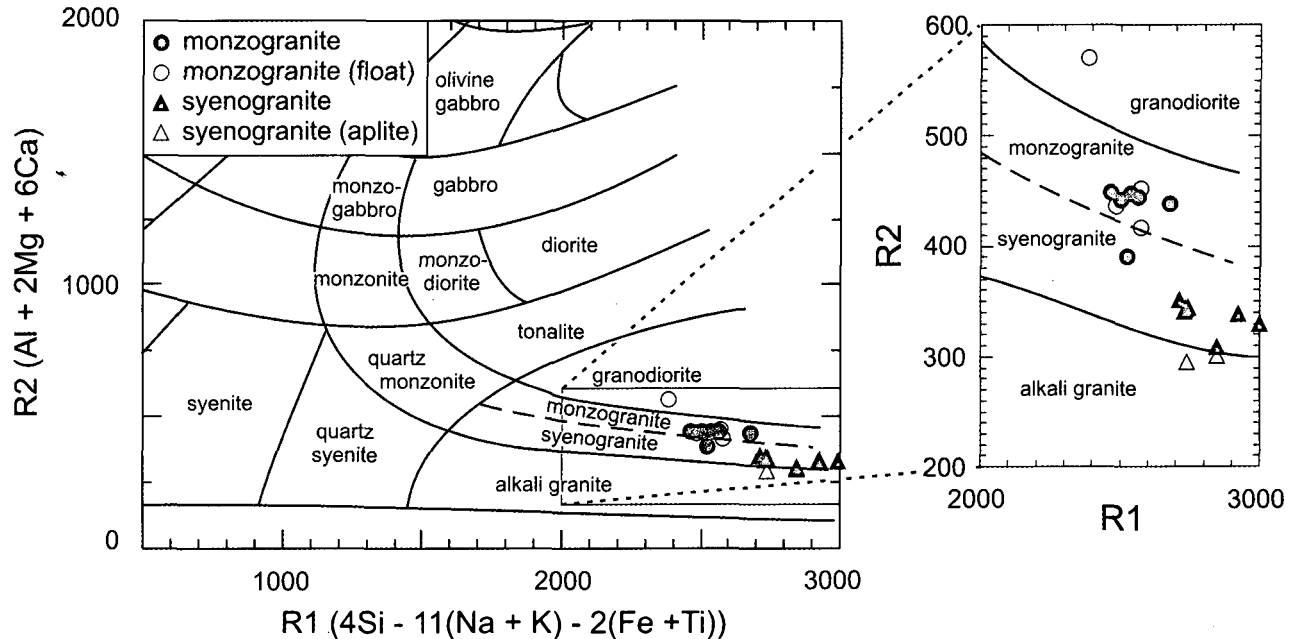

Fig. 6. Chemical classification of the Whale Lake monzogranite and New Cornwall syenogranite (nomenclature of de la Roche *et al.* 1980).

the original compositions of the monzogranite and syenogranite have not been greatly affected by alteration.

The New Cornwall syenogranite is lower in Al_2O_3, TiO_2, MgO, CaO, $Fe_2O_3^t$, Ba, Sr, Y, Zr and Nb, slightly higher in Rb, and higher in K_2O, compared to the Whale Lake monzogranite (Figs. 7 and 8). In some plots of elements against SiO_2 (Figs. 7, 8) syenogranite shows linear trends similar to the monzogranite (TiO_2, ?MgO, CaO, $Fe_2O_3^t$, Ba, Sr, Zr, Nb), in others (Na_2O, K_2O, MnO, ?P_2O_5, ?Rb and Y) the two rocks types form distinct clusters.

Fig. 9 compares the rocks of this study to magmatic trends in the SMB defined by Clarke *et al.* (1993) from average compositions of granodiorite, monzogranite and leucomonzogranite. Both the Whale Lake monzogranite and the New Cornwall syenogranite have A/CNK from 1.2 to 1.3,

with one value of 1.4 in one syenogranite. These values are, in general, greater than the magmatic trend of Clarke *et al.* (1993).

The K/Rb ratio (Fig. 9b) for the Whale Lake monzogranite ranges from 177 to 209 (Table 2) and for the New Cornwall syenogranite from 196 to 224. Although the average Rb content of the syenogranite is slightly higher than the monzogranite, they both show essentially the same range of Rb contents (180–210 ppm). In contrast, most of the analyses of "associated" and all analyses of "independent" leucogranite by Clarke *et al.* (1993) have much higher Rb, with K/Rb ratios of <180. Even average muscovite – biotite monzogranite and leucomonzogranite have K/Rb of <160. A similar contrast is seen on a plot of Rb vs. Ba (Fig. 9d), where both monzogranite and syenogranite samples lie on a straight
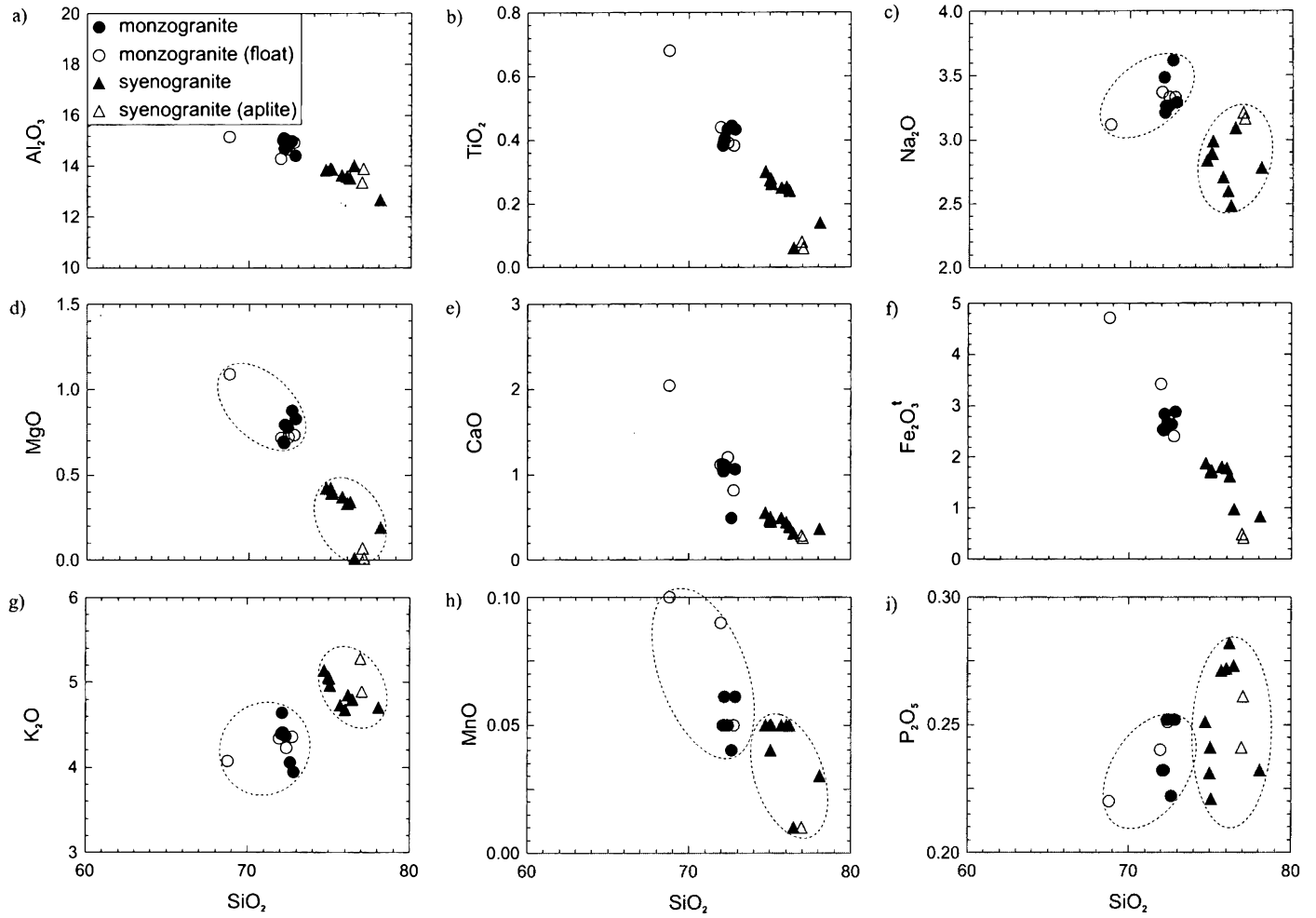
Fig. 7. Selected major elements plotted against SiO₂ (wt. %). Dashed lines outline clusters of monzogranite and syenogranite.
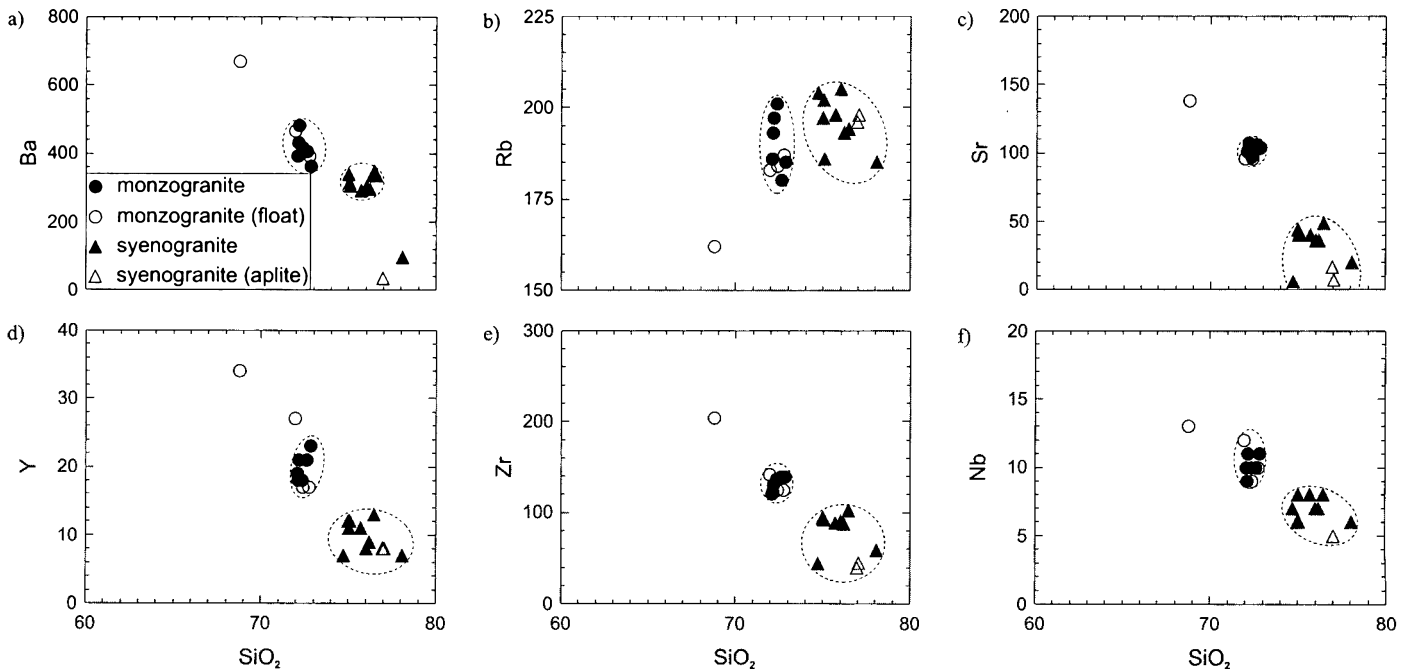
Fig. 8. Selected trace elements (ppm) plotted against SiO₂ (wt. %). Dashed lines outline clusters of monzogranite and syenogranite.

Fig. 9. Chemical variation diagrams for selected major and trace elements. The heavy line on each of these diagrams with the arrowhead indicates the direction of increasing differentiation by crystal-melt separation and is taken from Clarke *et al.* (1993). (For TiO₂, Clarke *et al.* trend has been corrected from their Fig. 4c after changing 1.75 to 0.75% TiO₂).

Table 2. Chemical analyses of representative granitoid rocks

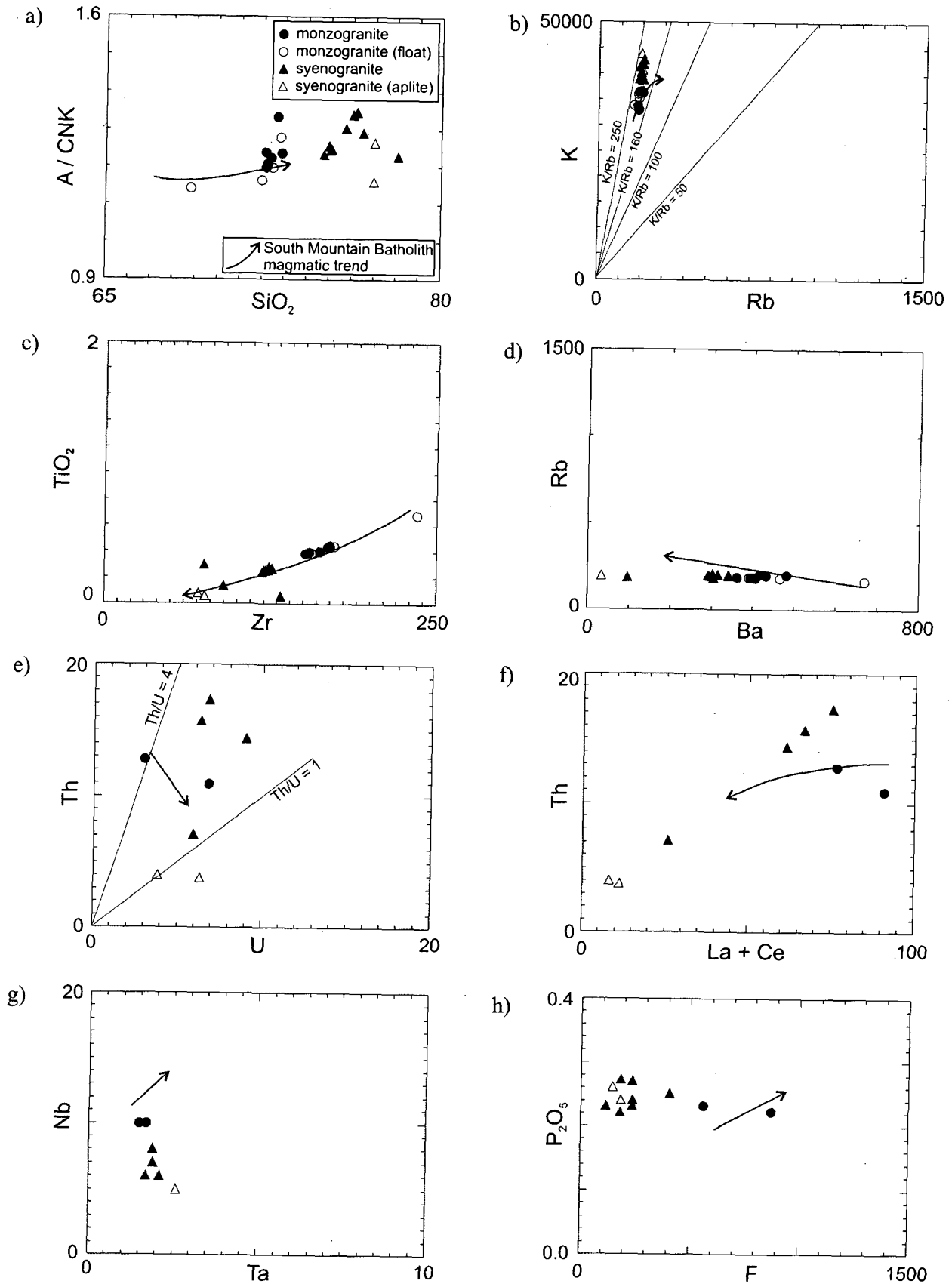| Rock Type Sample	DCmg DL001	DCmg DL003A	DCmg DL003B	DCmg DL004	DCmg DL004A	DCmg[1] DL005	DCmg[1] DL008F	DCmg[1] DL009A	DCmg[1] DL010	DCsg DL012B	DCsg DL013	DCmg DL014	DCsg DL015	DCsg DL015A	DCsg DL016	DCsg DL017	DCsg DL019	DCsg[2] DL022A	DCsg DL022	DCsg DL023	DCsg[2] DL025A
SiO_2	71.85	71.56	72.12	71.39	71.71	72.14	71.94	68.65	72.14	74.50	74.70	71.59	77.55	75.57	75.28	74.49	74.49	75.76	76.63	74.79	76.55
TiO_2	0.44	0.40	0.43	0.39	0.43	0.38	0.44	0.68	0.39	0.27	0.26	0.38	0.14	0.25	0.25	0.30	0.30	0.06	0.06	0.28	0.08
Al_2O_3	14.84	14.58	14.26	14.96	14.64	14.80	14.31	15.13	14.63	13.82	13.81	14.90	12.59	13.49	13.56	13.81	13.81	13.87	13.83	13.81	13.29
Fe_2O_3[1]	2.61	2.82	2.85	2.50	2.62	2.39	3.43	4.70	2.72	1.72	1.72	2.52	0.83	1.77	1.79	1.87	1.87	0.97	0.42	1.70	0.49
MnO	0.04	0.06	0.06	0.05	0.05	0.05	0.09	0.10	0.05	0.05	0.05	0.05	0.03	0.05	0.05	0.05	0.05	0.01	0.00	0.04	0.01
MgO	0.87	0.79	0.82	0.68	0.77	0.73	0.72	1.09	0.72	0.42	0.40	0.69	0.19	0.33	0.37	0.42	0.42	0.01	0.01	0.39	0.07
CaO	0.49	1.11	1.06	1.03	1.07	0.81	1.12	2.04	1.20	0.46	0.45	1.11	0.36	0.44	0.49	0.55	0.55	0.31	0.26	0.50	0.28
Na_2O	3.58	3.23	3.26	3.18	3.23	3.30	3.37	3.11	3.32	2.87	2.97	3.46	2.76	2.58	2.69	2.83	2.83	3.06	3.15	2.88	3.19
K_2O	4.02	4.37	3.91	4.60	4.33	4.32	4.34	4.07	4.21	5.03	4.94	4.36	4.67	4.65	4.70	5.12	5.12	4.75	4.87	5.03	5.25
P_2O_5	0.22	0.23	0.25	0.23	0.25	0.25	0.24	0.22	0.25	0.23	0.22	0.23	0.23	0.27	0.27	0.25	0.25	0.27	0.26	0.24	0.24
L.O.I.	1.31	0.91	0.99	0.88	0.86	0.95	0.62	0.54	0.67	0.76	0.79	0.67	0.61	0.91	0.88	0.70	0.70	0.85	0.74	0.74	0.55
Total	100.27	100.06	100.01	99.89	99.96	100.12	100.62	100.33	100.30	100.13	100.31	99.96	99.96	100.31	100.33	100.39	100.39	99.92	100.23	100.40	100.00
Trace elements (ppm)[3]																					
Ba	406	482	362	432	417	391	465	670	403	340	305	393	97	302	292	b.d.	295	342	b.d.	315	34
Rb	180	197	185	193	201	187	183	162	184	197	186	186	185	205	198	204	193	194	198	202	196
Sr	106	107	104	102	97	103	96	138	96	44	42	101	20	36	40	6	36	49	7	40	17
Y	21	21	23	18	18	17	27	34	17	12	12	19	7	8	11	7	9	13	8	11	8
Zr	139	131	139	123	137	125	142	204	125	95	92	120	59	90	89	44	88	102	45	93	40
Nb	10	11	11	9	10	10	12	13	9	6	6	10	6	7	8	7	7	8	5	8	b.d.
Th	10	11	b.d.	10	13	11	b.d.	11	14	15	12	11	12	20	12	10	15	15	b.d.	16	b.d.
Pb	17	18	16	18	15	15	19	21	15	22	19	19	17	19	16	17	18	20	16	19	19
Ga	16	15	17	19	20	19	18	17	18	17	15	18	16	19	18	23	19	16	23	18	16
Zn	33	38	56	27	43	23	52	56	50	22	19	45	7	16	23	8	10	28	b.d.	20	b.d.
Cu	16	33	48	41	60	10	6	8	38	45	44	b.d.	15	34	98	316	59	6	10	79	b.d.
Ni	b.d.	8	10	b.d.	8	7	8	13	6	b.d.	b.d.	8	b.d.	b.d.	b.d.	b.d.	b.d.	5	b.d.	6	b.d.
V	31	30	31	25	33	27	27	52	23	13	12	26	5	14	12	b.d.	13	13	5	11	b.d.
Cr	23	28	30	29	27	30	29	46	26	13	15	24	10	19	18	9	18	18	11	20	7
F	874	n.d.	n.d.	n.d.	n.d.	n.d.	n.d.	n.d.	n.d.	235	183	560	115	n.d.	235	408	n.d	145	183	235	183
Li	70	n.d.	n.d.	n.d.	n.d.	n.d.	n.d.	n.d.	n.d.	69	67	99	32	n.d.	64	78	n.d	15	19	71	17
REE and other trace elements (ppm) by INAA																					
La	27.70	n.d.	n.d.	n.d.	n.d.	n.d.	n.d.	n.d.	n.d.	20.70	n.d.	23.50	7.69	n.d.	18.20	23.10	n.d.	2.12	n.d.	n.d.	3.18
Ce	63.00	n.d.	n.d.	n.d.	n.d.	n.d.	n.d.	n.d.	n.d.	46.00	n.d.	53.00	18.00	n.d.	43.00	52.00	n.d.	6.00	n.d.	n.d.	8.00
Nd	29.00	n.d.	n.d.	n.d.	n.d.	n.d.	n.d.	n.d.	n.d.	24.00	n.d.	25.00	10.00	n.d.	21.00	28.00	n.d.	4.00	n.d.	n.d.	6.00
Sm	5.03	n.d.	n.d.	n.d.	n.d.	n.d.	n.d.	n.d.	n.d.	5.82	n.d.	5.80	2.38	n.d.	5.28	6.34	n.d.	1.29	n.d.	n.d.	1.49
Eu	0.86	n.d.	n.d.	n.d.	n.d.	n.d.	n.d.	n.d.	n.d.	0.38	n.d.	0.78	0.16	n.d.	0.34	0.42	n.d.	0.06	n.d.	n.d.	0.09
Tb	0.80	n.d.	n.d.	n.d.	n.d.	n.d.	n.d.	n.d.	n.d.	0.60	n.d.	0.60	0.40	n.d.	0.40	0.60	n.d.	0.20	n.d.	n.d.	0.20
Yb	2.13	n.d.	n.d.	n.d.	n.d.	n.d.	n.d.	n.d.	n.d.	1.01	n.d.	1.63	0.73	n.d.	0.87	1.01	n.d.	0.75	n.d.	n.d.	0.79
Lu	0.32	n.d.	n.d.	n.d.	n.d.	n.d.	n.d.	n.d.	n.d.	0.15	n.d.	0.25	0.11	n.d.	0.12	0.14	n.d.	0.11	n.d.	n.d.	0.11
Co	50.00	n.d.	n.d.	n.d.	n.d.	n.d.	n.d.	n.d.	n.d.	63.70	n.d.	52.10	97.10	n.d.	66.90	74.20	n.d.	88.40	n.d.	n.d.	139.00
Cs	10.90	n.d.	n.d.	n.d.	n.d.	n.d.	n.d.	n.d.	n.d.	15.00	n.d.	13.30	7.10	n.d.	12.30	13.50	n.d.	7.90	n.d.	n.d.	10.20
Hf	4.40	n.d.	n.d.	n.d.	n.d.	n.d.	n.d.	n.d.	n.d.	3.30	n.d.	4.20	2.20	n.d.	3.20	3.70	n.d.	2.10	n.d.	n.d.	1.70
Sc	7.37	n.d.	n.d.	n.d.	n.d.	n.d.	n.d.	n.d.	n.d.	3.85	n.d.	6.11	1.79	n.d.	3.69	4.28	n.d.	2.44	n.d.	n.d.	1.40
Ta	1.50	n.d.	n.d.	n.d.	n.d.	n.d.	n.d.	n.d.	n.d.	1.70	n.d.	1.70	2.10	n.d.	1.90	1.90	n.d.	2.60	n.d.	n.d.	2.30
Th	10.90	n.d.	n.d.	n.d.	n.d.	n.d.	n.d.	n.d.	n.d.	15.70	n.d.	12.80	7.10	n.d.	14.40	17.30	n.d.	4.00	n.d.	n.d.	3.80
U	6.80	n.d.	n.d.	n.d.	n.d.	n.d.	n.d.	n.d.	n.d.	6.30	n.d.	3.00	5.90	n.d.	9.00	6.80	n.d.	3.80	n.d.	n.d.	6.30
A/CNK[4]	1.3	1.2	1.2	1.2	1.2	1.3	1.2	1.2	1.2	1.3	1.3	1.2	1.2	1.3	1.3	1.2	1.4	1.3	1.3	1.3	1.2
K/Rb	187	186	177	200	186	193	197	209	191	213	222	196	211	190	198	209	209	205	209	207	224
Nb/Ta	6.7	n.d.	n.d.	n.d.	n.d.	n.d.	n.d.	n.d.	n.d.	3.5	n.d.	5.9	2.9	n.d.	4.2	3.7	n.d.	3.1	n.d.	n.d.	n.d.

Notes: DCmg = Whale Lake monzogranite; DCsg = New Cornwall syenogranite; b.d. = below detection limit; n.d. = not determined; [1]float; [2]aplite; [3]All trace elements (in ppm) by XRF except Li (atomic absorption) and F (specific ion electrode). [4]A/CNK = mol{Al_2O_3 / (CaO + Na_2O + K_2O)}
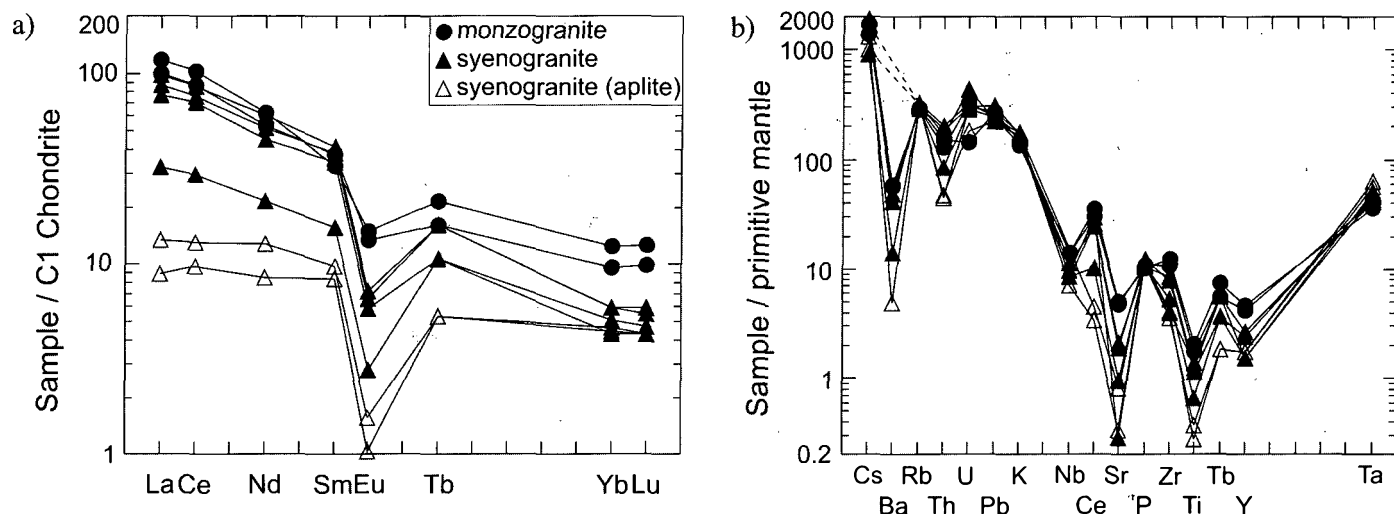
Fig. 10. (a) REE abundances normalized to C1 chondrite. (b) Trace element abundances normalized to primitive mantle (Sun and McDonough 1989).

line of almost constant Rb with quite variable Ba.

The monzogranite and syenogranite form a clear linear trend on a TiO_2 vs. Zr plot (Fig. 9c), identical to the trend defined by MacDonald *et al.* (1992) and Clarke *et al.* (1993). A plot of Th vs. U shows a wide scatter (Fig. 9e). A plot of Th vs. La + Ce (Fig. 9f) shows a linear trend for syenogranite and aplite that has higher Th than the SMB magmatic trend. The monzogranite shows scatter around the magmatic trend. The syenogranite has lower Nb/Ta values (ave. 3.5) than the monzogranite (ave. 6.3) and both plot a little below the SMB magmatic trend of Clarke *et al.* (1993) (Fig. 9g). Fluorine content of the Whale Lake monzogranite is similar to that of average SMB monzogranite (Fig. 9h), but fluorine content of the New Cornwall syenogranite is unusually low (<450 ppm) compared with SMB rocks (typically 500–1000 ppm).

The Whale Lake monzogranite shows high ΣREE, greater fractionation of LREE than HREE, and a small Eu anomaly (Fig. 10a). In these respects, it is very similar to the early magmatic rocks of the SMB. Although two of the analyzed syenogranite samples overlap in LREE with the monzogranite, they have lower HREE. One syenogranite has much lower ΣREE and the ΣREE of the aplite is still lower (Fig. 10a). The Eu anomaly in all the syenogranite and aplite samples is similar, and significantly greater than in the monzogranite. Incompatible trace elements are slightly less abundant in the New Cornwall syenogranite than in the Whale Lake monzogranite (Fig. 10b). In particular, both rock types show strong relative depletion in Ba, Th, Nb, Sr and Ti compared with other incompatible elements.

Elements such as Ti, Fe, Mn, Ca, P, Ba, Rb, Sr, and Zr are more indicative of the degree of differentiation than either SiO_2 or Thornton and Tuttle's (1960) differentiation index, and ratios of these elements are even more sensitive (Whalen 1980). Ratios using Rb, Ba, and Sr are the most useful, because these elements occur almost solely in the major silicate minerals of granitoids, but they are potentially mobile. On the other hand elements such as Ti and Zr are considered to be less mobile during alteration (Floyd and Winchester 1975), although they could be concentrated in accessory minerals. When plotted on two-element diagrams (Fig. 11),

the patterns shown by the Whale Lake monzogranite and New Cornwall syenogranite are not inclined straight-line distributions. These patterns (Fig. 11) plot as vertical straight lines. An inclined straight-line pattern, particularly on log-log plots, is considered the result of fractional crystallization. The observed vertical straight-line distribution suggests alteration has not been significant. The reason for the almost constant Rb/P ratio is unclear, since Rb is principally in mica, whereas P is in apatite.

Nd isotopes

Nd/Sm isotopes were determined on five samples: two monzogranite, two syenogranite and one mineralized syenogranite (Table 3). The Nd/Sm systematics in the mineralized syenogranite appear disturbed, with a low Sm/Nd ratio. The other four samples show similar values of ε_{Nd} between -1.8 and -2.2 and similar values of model age (t_{DM} of 1.3 to 1.5 Ga).

Table 3. Sm and Nd isotope compositions of the New Cornwall area granitoid rocks.

Sample	Sm ppm	Nd ppm	$\frac{^{147}Sm}{^{144}Nd}$	$\frac{^{143}Nd}{^{144}Nd}$	Age (Ga)	ε_{Nd} initial	T_{DM} (Ga)
Monzogranite							
DL001	5.97	27.19	0.1328	0.51237	0.37	-2.17	1.27
DL014	6.28	27.30	0.1391	0.51240	0.37	-1.92	1.31
Syenogranite							
DL012	4.83	27.97	0.1043	0.51243	0.37	0.31	0.89
DL017	6.93	27.48	0.1525	0.51243	0.37	-1.99	1.50
DL020	6.89	27.50	0.1485	0.51243	0.37	-1.78	1.42

Notes: For T_{DM} ages determinations, the equation used is that of Faure (1986). For ε_{Nd} determinations constants used were $^{143}Nd/^{144}Nd = 0.512638$, $^{147}Sm/^{144}Nd = 0.1967$ and an assumed age of 0.37 Ga.
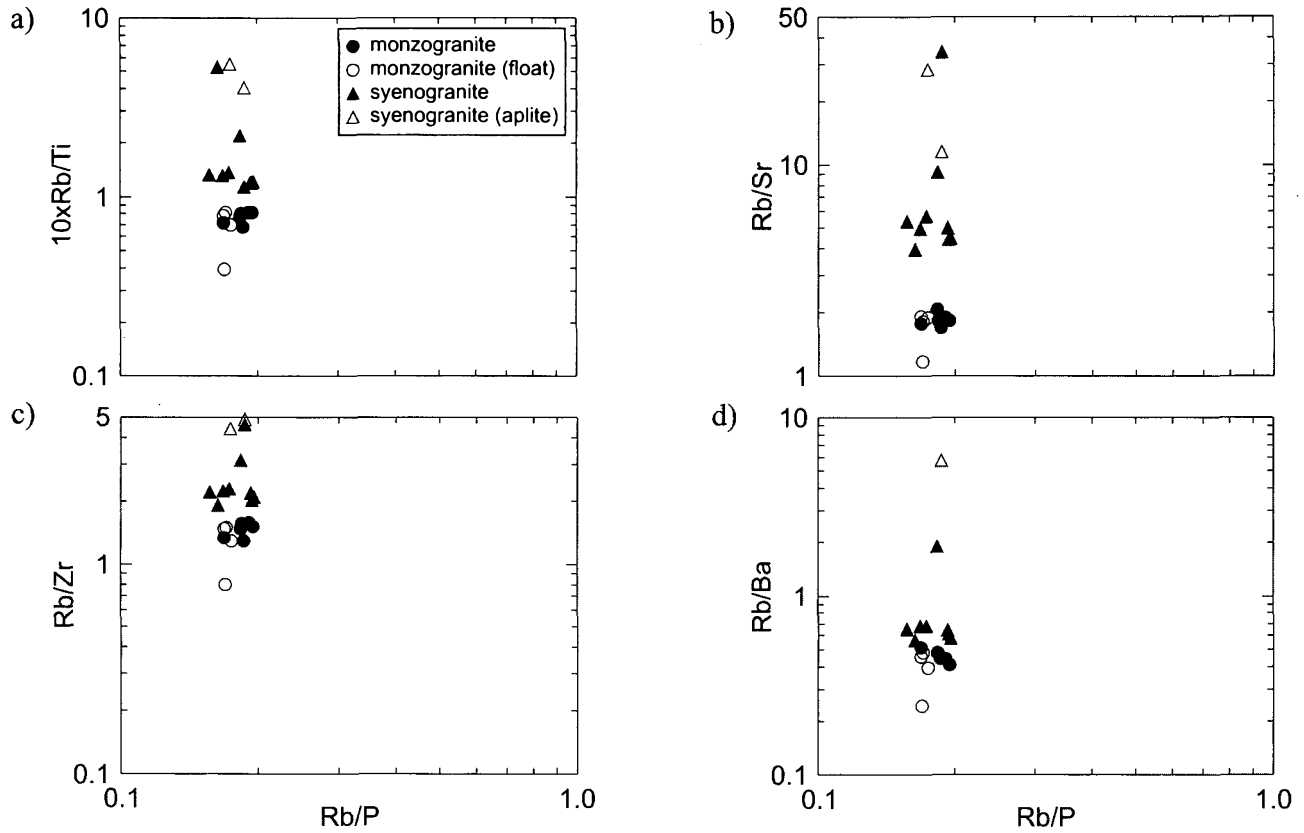
Fig. 11. Selected element ratios plotted against the Rb/P ratio (log scales).

Fig. 12. Ternary variation in An, Ab, Or of the analysed feldspars from both the monzogranite and the syenogranite.

MINERAL CHEMISTRY

Feldspar

Plagioclase is ubiquitous in both monzogranite and syenogranite. The plagioclase (Fig. 12) present in the monzogranite ranges from albite to andesine (An_{2-35}) and in the syenogranite from albite to the boundary separating andesine from oligoclase (An_{1-29}). Although the upper limit of the An content in the monzogranite is higher, the compositional difference in plagioclase between the syenogranite and the monzogranite is not great (< 6 An mol. %, Fig. 13). Most of the plagioclase in both the monzogranite and syenogranite has normal zoning (83% of the studied crystals in the monzogranite and 79% in the syenogranite), some are reversely zoned (about 17% of the studied crystals in both), and only rarely is zoning absent.

K-feldspar is also ubiquitous in both the monzogranite and syenogranite. The compositional range in the monzogranite is Or_{88-95} and in the syenogranite Or_{81-95}. The differences between the two, as seen in Fig. 13, are: 1) The syenogranite shows greater range of Or mol. %, mainly in the lower end and 2) the compositional range of the K-feldspar crystal cores in the monzogranite is greater than that in the rims. Most of the studied crystals in the monzogranite are reversely zoned (63%) and only 38% show normal zoning. In contrast, in the syenogranite 67% of the crystals studied show normal zoning, 29% reverse, and only 4% are not zoned.
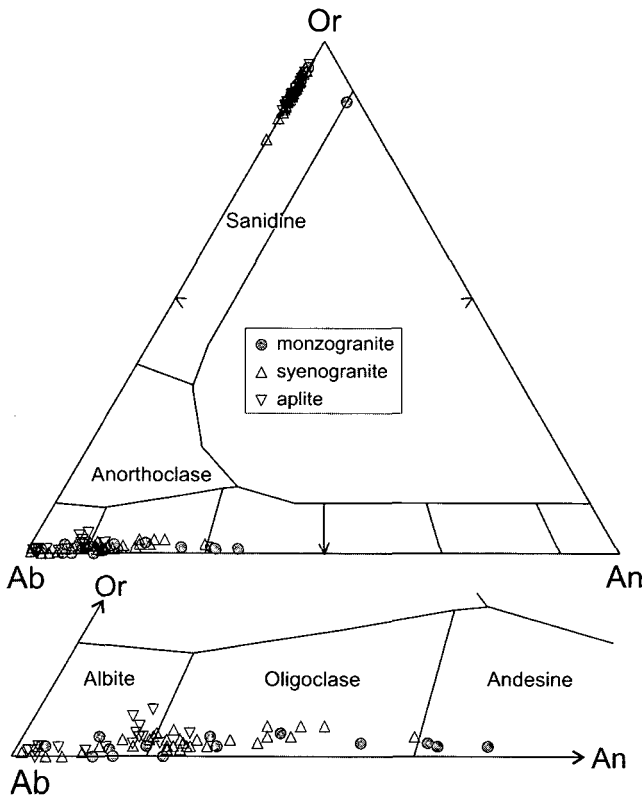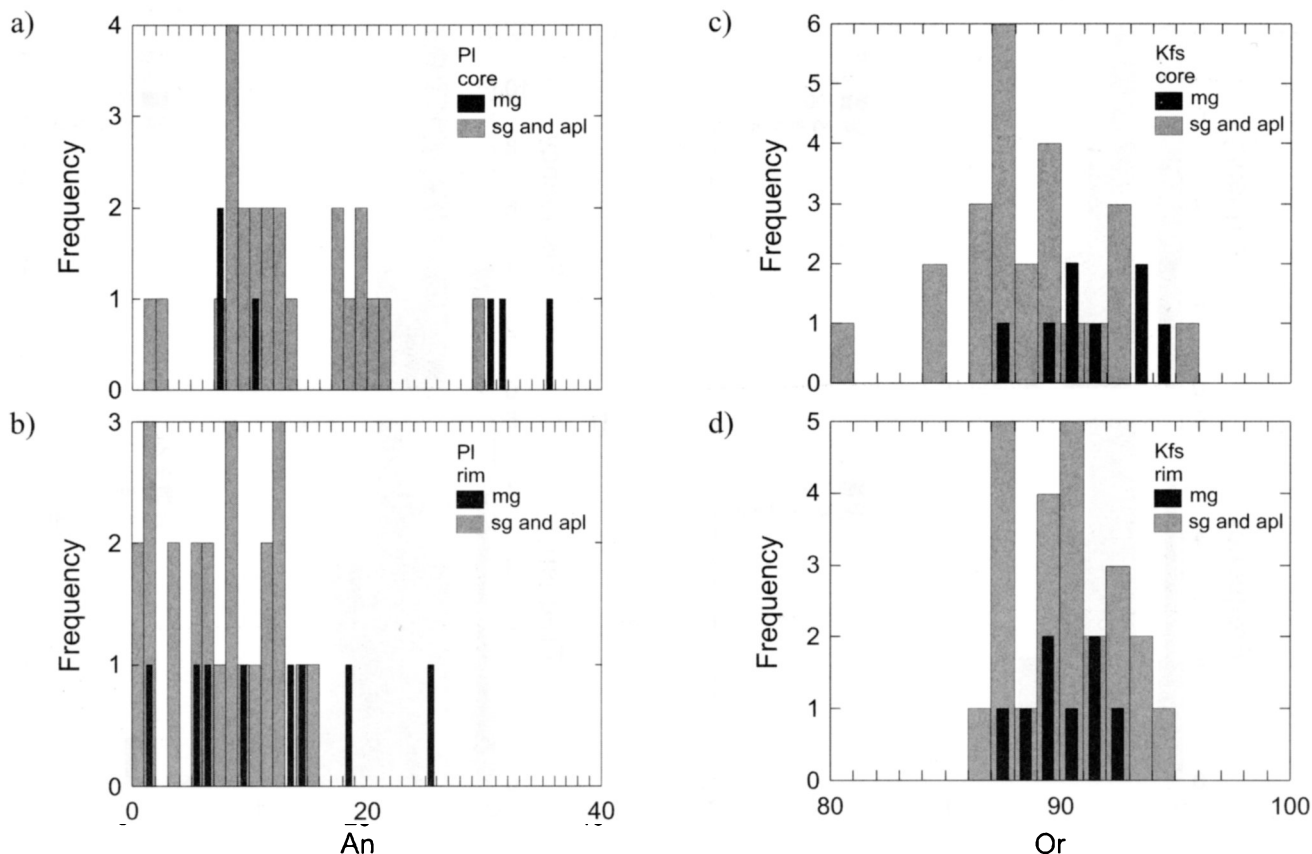
Fig. 13. Histogram of An (mol. %) for cores and rims of plagioclase (a and b) and Or (mol. %) for cores and rims of alkali-feldspar (c and d) from the Whale Lake monzogranite and the New Cornwall syenogranite. Abbreviations: mg, monzogranite; sg, syenogranite; apl, aplite; pl: plagioclase; Kfs: K-feldspar.

The range of P_2O_5 concentrations in the both plagioclase and K-feldspar cores is generally similar in the monzogranite and syenogranite (Fig. 14a, c), whereas the rims of both feldspars in the syenogranite have higher P_2O_5, particularly in K-feldspar (Fig. 14d). Apatite is a common primary accessory mineral in the monzogranite, occurring as interstitial subhedral to euhedral crystals up to 0.2 mm in diameter, in contact with biotite, feldspars, and quartz. No apatite crystals were found in the syenogranite or aplite, either interstitially or as inclusions in other minerals. Plagioclase from the syenogranite shows no evidence of alteration (note the uniform Na and Ca distribution in Figs. 15c, d). There is certainly no patchy alteration by P-rich fluids (as postulated for leucogranite by Clarke et al. 1993) and only very rarely are apatite microlites found near the rims (Fig. 15b).

Biotite

Biotite is ubiquitous in the monzogranite and the syenogranite, but is absent from aplite. Analyses from both rock types fall in the range of peraluminous rocks recognized by Abdel-Rahman (1994) (Fig. 16a). In some samples, Fe content increases significantly towards the rim (Table 4).

Muscovite

Using thin section textural criteria described by Saavedra (1978) and Ham and Kontak (1988), both primary (magmatic) and secondary muscovite are present in monzogranite and syenogranite. When Ti–Na–Mg is plotted for muscovite (Fig. 16b), some of the analyses from the monzogranite fall in the field for primary muscovite as defined by Miller et al. (1981), whereas many analyses from monzogranite and all analyses of muscovite from syenogranite fall in the field for secondary muscovite, except for some muscovite overgrowths on andalusite discussed below. Ham and Kontak (1988) found that primary muscovite from more leucocratic rocks of the SMB had extremely low Ti (i.e. secondary muscovite in the classification of Miller et al. 1981). We therefore place more reliance on petrographic character, which suggests that about 25% of the muscovite in the syenogranite is primary. In most crystals, Fe content decreases towards the rim, but in a few, the opposite trend is observed (Table 5).

Tourmaline

Tourmaline is an accessory mineral in the syenogranite and occurs in trace amounts in some monzogranite samples. It occurs as subhedral to euhedral crystals 0.1 mm to 2.2 mm in length, although most crystals are small and average 0.5 mm. Crystals are pleochroic from green to yellow and reddish, with
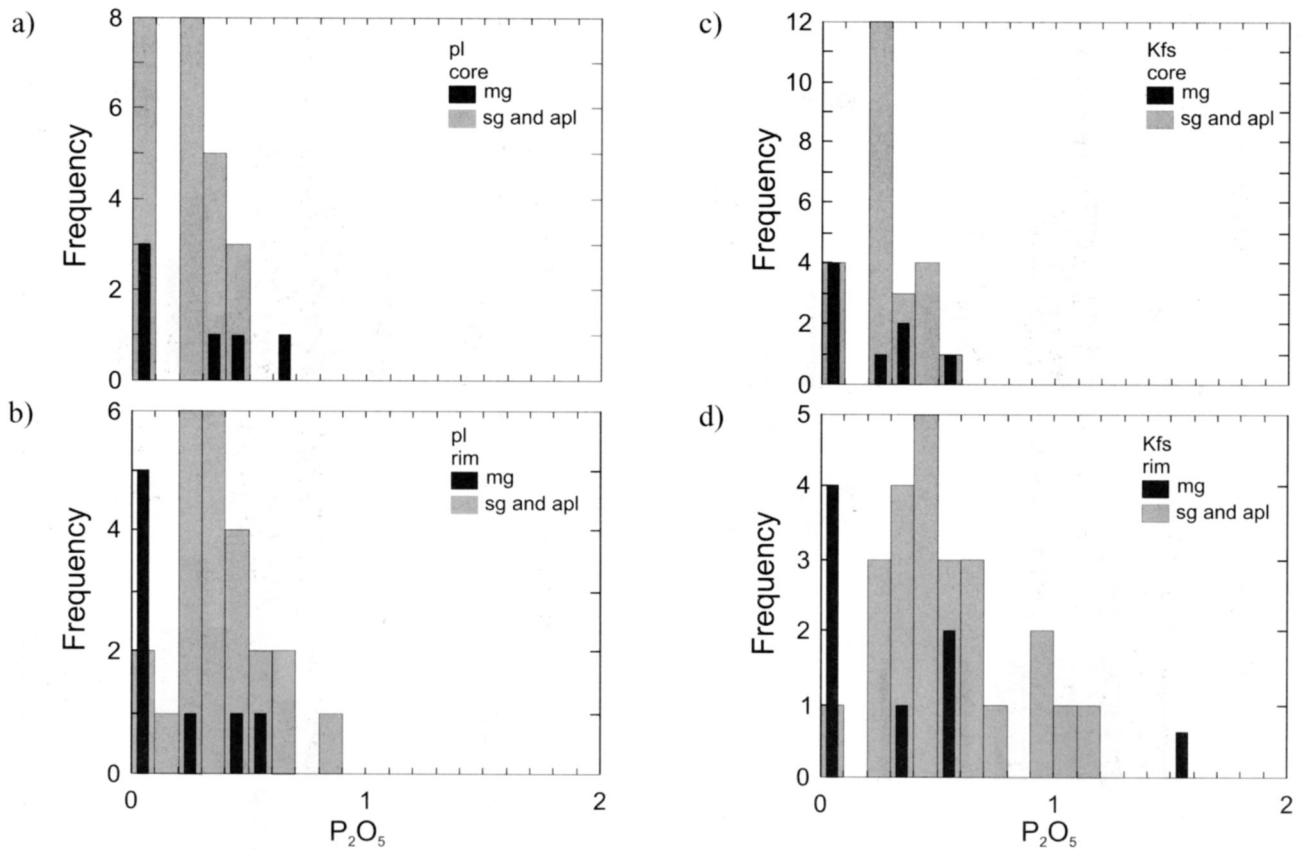
Fig. 14. Histogram of P_2O_5 (wt. %) for cores and rims of feldspars from the Whale Lake monzogranite and the New Cornwall syenogranite. Abbreviations as in Fig. 13.
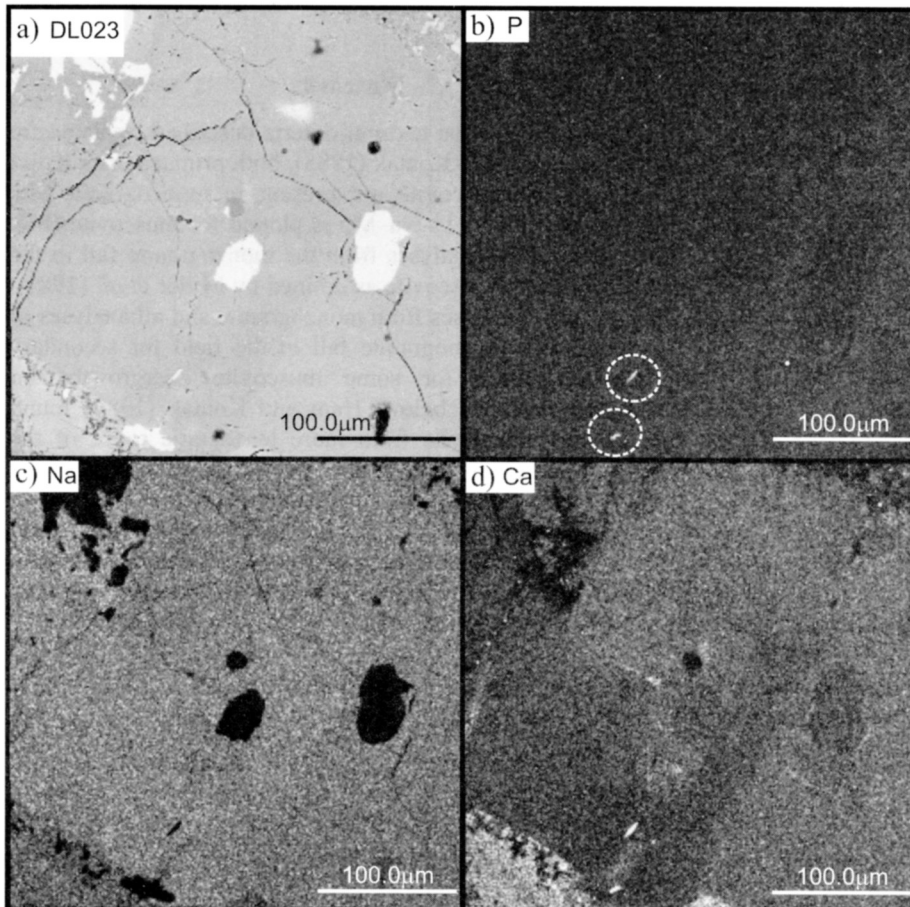

Fig. 15. Images of identical areas of a plagioclase crystal from syenogranite showing (a) back-scattered electron image, (b) X-ray map for P showing absence of patchy alteration and rare apatite microlites (circles), (c) X-ray map for Na, and (d) X-ray map for Ca.

Table 4. Representative chemical analyses of biotite

Rock Type Sample Position	DCmg DL003 1-core	DCmg DL003 1-rim	DCmg DL004A 2-core	DCmg DL004A 2-rim	DCsg DL013 3-core	DCsg DL013 3-rim	DCsg DL013 4-core	DCsg DL013 4-rim	DCsg DL013 5-core	DCsg DL013 5-rim
SiO_2	35.52	34.94	36.06	35.44	35.99	35.69	35.55	35.17	35.43	35.34
TiO_2	4.09	3.79	0.00	0.00	1.50	1.18	2.53	2.63	3.95	3.65
Al_2O_3	18.91	18.55	20.06	19.91	20.43	20.76	19.17	19.31	19.14	19.46
FeO^t	20.70	20.62	17.82	19.07	20.11	20.11	20.46	21.38	21.89	21.33
MnO	0.45	0.43	0.41	0.36	0.55	0.73	0.48	0.60	0.44	0.00
MgO	7.26	7.56	10.36	10.03	8.00	8.04	7.47	7.01	6.31	6.34
Na_2O	0.34	0.28	0.00	0.00	0.00	0.31	0.00	0.00	0.38	0.28
K_2O	9.54	8.79	9.51	9.54	9.39	9.52	9.38	9.42	9.33	9.42
Total	96.81	94.96	94.22	94.35	95.97	96.34	95.04	95.52	96.87	95.82

the normal pleochroism of the tourmaline commonly masked by chloritization and staining. Minerals in contact with tourmaline include plagioclase, quartz, and muscovite and its mode of occurrence indicates late magmatic precipitation. Tourmaline analyses from the syenogranite show increases in Al_2O_3 and Fe_2O_3 and decrease in MnO towards the rim (Table 6). Using the classification of Henry and Guidotti (1985), based on Al–Fe–Mg and Ca–Fe–Mg abundances (not shown here), the tourmaline from the syenogranite falls in their field 2 (Li-poor granitoids and associated pegmatite and aplite). Late magmatic tourmaline elsewhere in the SMB occurs only in aplite and pegmatite dykes or in xenolithic clots, where assimilated xenoliths are probably the source of the boron.

Andalusite

Andalusite was found only in the syenogranite and aplite. It occurs as small (average 0.5 mm in diameter), interstitial, subhedral to euhedral grains, which are pleochroic from colourless to pinkish. Most grains lack inclusions, although some contain small inclusions of zircon. The andalusite is essentially a pure phase, with iron being the most abundant minor element (FeO^t = 0.3–0.4%, Table 6). Both the mineralogical characteristics and chemistry are very similar to those assigned to magmatic (granitic) andalusite in the SMB by Clarke et al. (1976). MacDonald et al. (1992) noted that andalusite was found only in fine-grained leucomonzogranite and leucogranite.

Andalusite crystals are commonly mantled by anhedral muscovite and the petrographic evidence indicates a reaction relationship between andalusite and muscovite. The majority of the chemical analyses of muscovite overgrowths, when plotted in the Ti–Na–Mg diagram (Fig. 16b), fall in the field for primary muscovite after Miller et al. (1981). Such a relationship between primary muscovite and andalusite, following the argument of Clarke et al. (1976), may indicate pressures of 3.3 to 3.9 kb and temperatures of 710–660°C for the syenogranite.
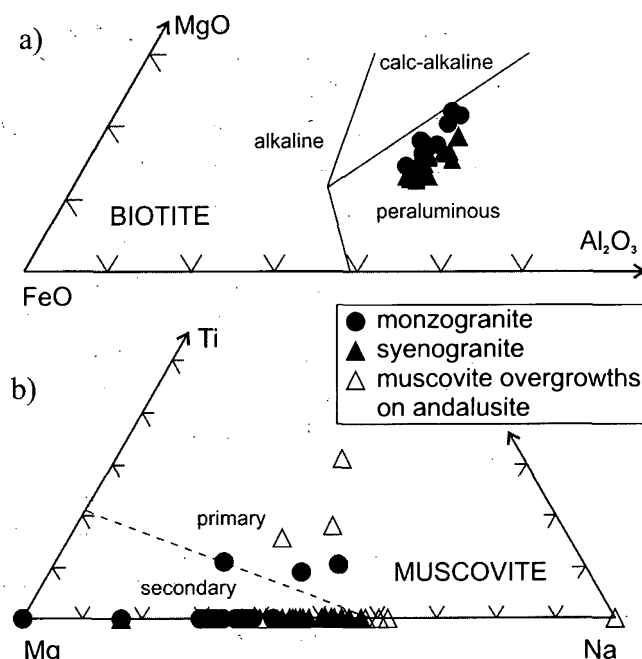

Fig. 16. Plots illustrating chemical variation in micas. a) Ternary variation for MgO, FeO, and Al_2O_3 in biotite. Alkaline (A), calc-alkaline (C), and peraluminous (P) fields are from Abdel-Rahman (1994). b) Ternary variation for Ti, Mg, and Na in muscovite, with primary and secondary fields after Miller et al. (1981)

Garnet

Garnet has been identified only in the Whale Lake monzogranite. The garnet crystals are colourless, subhedral to euhedral, small (<0.1–0.5 mm in diameter) and associated with biotite, and to a lesser extent plagioclase. Most garnet crystals lack inclusions, although some contain small zircon grains. The analysed garnet crystals (Table 6) are almandine in composition and on the Mn–Mg–Fe diagram (not shown here) they plot in the field of magmatic garnet after Allan and Clarke (1981).

Table 5. Representative chemical analyses of muscovite

| Rock Type | DCmg | DCmg | DCmg | DCmg | DCmg | DCmg | DCsg | DCsg | DCsg | DCsg | DCsg | DCsg |
| Sample | DL003 | DL003 | DL003 | DL003 | DL003 | DL003 | DL013 | DL013 | DL013 | DL013 | DL015 | DL015 |
Position	1-core	1-rim	2-core	2-rim	3-core	3-rim	1-core	1-rim	2-core	2-rim	B1[1]	B2[1]
SiO_2	47.19	47.71	47.91	47.51	48.33	47.04	46.75	47.39	47.46	47.88	47.28	46.36
TiO_2	0.31	0.00	0.00	0.00	0.00	0.00	0.00	0.00	0.00	0.00	0.37	0.00
Al_2O_3	37.20	36.84	35.09	33.96	36.88	36.36	36.20	37.01	36.98	36.77	37.43	36.87
FeO^t	0.85	1.19	2.35	1.81	1.45	1.14	1.69	1.41	1.40	1.61	0.96	0.94
MgO	0.62	0.79	1.64	1.45	0.77	0.80	0.69	0.76	0.81	0.96	0.57	0.45
Na_2O	0.55	0.44	0.25	0.00	0.28	0.31	0.44	0.50	0.48	0.43	0.32	0.23
K_2O	9.56	9.80	8.86	10.22	7.39	7.80	9.18	8.83	9.05	8.92	9.28	9.58
Total	96.28	96.77	96.10	94.95	95.10	93.45	94.95	95.90	96.18	96.57	96.21	94.43

[1]Muscovite mantling andalusite

Table 6. Representative chemical analyses of tourmaline, garnet, chlorite, and andalusite

Rock Type	DCsg	DCsg	DCsg	DCsg	DCmg	DCmg	DCmg	DCsg	DCsg
Sample	DL013	DL013	DL013	DL013	DL003	DL003	DL003	DL022	DL022
Position	1-core	1-rim	2-core	2-rim	core				
Mineral	Tur	Tur	Tur	Tur	Grt	Chl	Chl	And	And
SiO_2	37.61	38.55	38.17	38.21	36.85	27.08	26.24	36.50	36.31
TiO_2	31.00	31.14	30.80	31.59	21.00	18.40	20.65	62.83	62.65
Al_2O_3	12.31	12.88	11.20	11.51	32.13	29.47	28.04	0.31	0.38
FeO^t	0.00	0.00	0.00	0.00	5.48	0.00	0.43	0.00	0.00
MnO	4.33	3.90	4.32	4.10	3.31	11.53	12.69	0.00	0.17
MgO	0.30	0.18	0.26	0.17	1.23	0.00	0.00	0.00	0.00
Na_2O	0.00	0.17	0.00	0.00	0.00	0.00	0.31	0.00	0.00
K_2O	0.54	0.64	0.92	0.74	0.00	0.25	0.00	0.00	0.00
Total	86.09	87.46	85.67	86.32	100.00	86.73	88.36	99.64	99.34

Mineral abbreviations: Tur = tourmaline; Grt = garnet; Chl = chlorite; And = andalusite

Opaque minerals

The Fe-Ti oxides identified in the syenogranite are ilmenite, hematite, and rutile (Table 7). The identified sulphides in the same rocks include pyrite and chalcopyrite (Table 8).

DISCUSSION

The New Cornwall syenogranite characteristically contains 0.5–4% biotite and thus straddles the boundary between leucogranite and leucomonzogranite in the nomenclature of MacDonald et al. (1992). Samples analysed by Horne (1987) are reported as containing 6–9% biotite. The difference in biotite content between the two studies may be a consequence of how chlorite, having no direct relationship to original biotite, was counted. The New Cornwall syenogranite differs from typical leucomonzogranite geochemically in having a mean SiO_2 content of 75.8%, compared with 73.9% (MacDonald et al. 1992) and falls in the syenogranite rather

than the monzogranite field in the de la Roche et al. (1980) classification.

The New Cornwall syenogranite differs in several important respects from the leucogranite bodies described by Clarke et al. (1993). In field occurrence, the 1.7 km[2] area of the syenogranite is an order of magnitude greater than that of "associated" leucogranite bodies. However, the New Cornwall

Table 7. Representative chemical analyses of ilmenite and rutile

| Rock Type | DCsg | DCsg | DCsg | DCsg | DCsg | DCsg |
| Sample | DL019 | DL019 | DL019 | DL019 | DL30(1) | DL30(2) |
Mineral	Ilm	Ilm	Rt	Rt	Ilm	Ilm
SiO_2	0.39	0.00	0.35	0.00	0.22	0.24
TiO_2	53.03	51.53	98.81	100.08	51.72	51.59
FeO^t	40.89	38.16	0.00	0.00	41.46	37.66
MnO	6.30	8.99	0.00	0.00	4.49	8.52
Nb_2O_5	0.00	1.99	1.32	0.00	0.00	0.00
Total	100.61	100.67	100.48	100.08	97.89	98.01

Mineral abreviations: Ilm = ilmenite; Rt = rutile

Table 8. Representative chemical analyses of pyrite, chalcopyrite and pyrrhotite

Rock Type Sample Mineral	DCmg DL003B Py	DCmg DL003B Po	DCmg DL009A Py	DCmg DL009A Ccp	DCsg DL30(1) Py	DCsg DL30(1) Py	DCsg DL30(2) Py
Fe	33.70	46.70	33.64	25.35	33.31	33.17	33.39
As	b.d.	b.d.	b.d.	b.d.	0.18	0.17	0.00
S	66.30	53.07	66.37	50.50	66.50	66.66	66.61
Cu	0.00	0.00	0.00	23.92	0.00	0.00	0.00
Si	0.00	0.23	0.00	0.24	0.00	0.00	0.00
Total	100.00	100.00	100.01	100.01	99.99	100.00	100.00

Mineral abbreviations: Py, pyrite; Po, Pyrrhotite; Ccp, chalcopyrite (as an inclusion in pyrite). b.d. = below detection limit

leucogranite is not highly fractionated: ratios such as A/CNK, Rb/K and Nb/Ta resemble the "associated" group. We therefore discuss below the processes that Clarke et al. (1993) have suggested played a role in the evolution of "associated" leucogranite.

How similar are the Whale Lake monzogranite and New Cornwall syenogranite, and could the syenogranite have developed from the monzogranite by open-system interaction with fluid (Clarke et al. 1993)? Similarities between the monzogranite and the syenogranite are indicated by regular trends in binary element plots such as the trend in TiO_2 vs. Zr (Fig. 9c) and Ba, Sr and Nb vs. SiO_2 (Fig. 8). Similarly regular trends have been observed in SMB rocks by MacDonald et al. (1992) and Clarke et al. (1993). The monzogranite and syenogranite differ from average SMB rocks in having slightly higher A/CNK, low Rb and low Nb. The monzogranite and syenogranite have identical values of ε_{Nd} to within analytical error (Fig. 17). This is in contrast with the wide range of ε_{Nd} (1.5 to -5) elsewhere in the SMB (Clarke et al. 1988). Some of this regional variability in the SMB results from differing degrees of assimilation of Meguma Group metasedimentary xenoliths (with $\varepsilon_{Nd} = -10$). This process appears insufficient to explain all the variability, which is therefore likely a consequence of partial melting of different lower to middle crustal source rocks (Pe-Piper and Jansa, 1999). Such a process was also inferred on geochemical grounds by MacDonald et al. (1992). The Nd isotopic data in the New Cornwall area suggest that monzogranite and syenogranite are related, either by fractionation, interaction with fluid, or partial melting, of the same source. The slight difference in model ages might also result from fractionation by accessory mineral phases in the source rock, as proposed by Ayres and Harris (1997).

One characteristic of the "associated" leucogranite bodies of Clarke et al. (1993) is that they show REE distributions very similar to the host monzogranite. The New Cornwall syenogranite has substantially different REE abundances with consistently lower Eu and HREE (Fig. 10) compared to the Whale Lake monzogranite. However, both the monzogranite and syenogranite have greater LREE abundances than any of the leucogranite bodies or their leuco- or monzogranite hosts
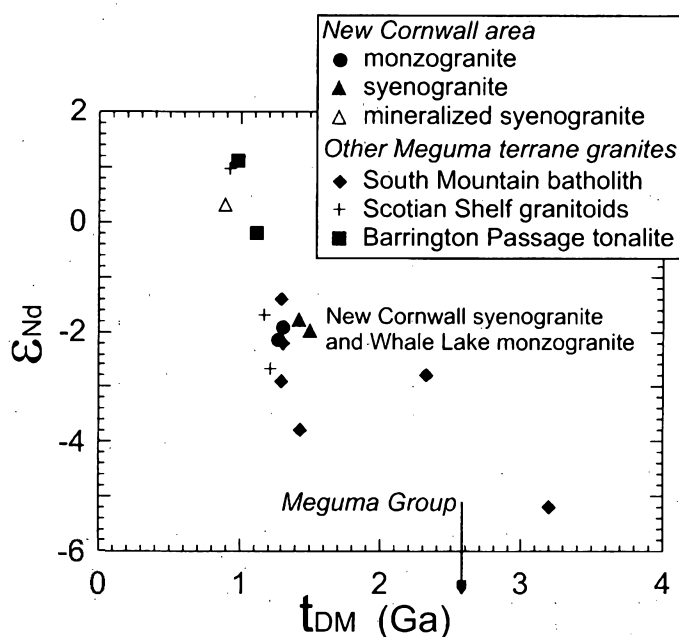

Fig. 17. ε_{Nd} vs. t_{DM} for t = 370 Ma. The sources of data for the other Meguma terrane granites are Clarke et al. (1988) and Pe-Piper and Jansa (1999)

described by Clarke et al. (1993), again pointing to similarities in origin between the two rock types in the New Cornwall area.

Several lines of evidence suggest that the New Cornwall syenogranite is not related to the Whale Lake monzogranite by fractionation. The lack of variation of Rb with Ba (Fig. 9d) suggests fractional crystallization of alkali feldspar was not a process relating the two groups of rocks. The variation of U with Th (Fig. 9e) is not consistent with the fractionation of minerals, such as a monazite, as the process responsible for the evolution of monzogranite to syenogranite. The average Th value for the monzogranite is 11 and for the syenogranite 14. If these two rock types were related through a process that included monazite fractionation, the Th content of the syenogranite should have been considerably lower than in the monzogranite. Likewise, the scatter in La + Ce vs. Th (Fig. 9f)

does not suggest fractionation of the syenogranite from the monzogranite.

The similarity in P_2O_5 contents in the cores of feldspars and the greater range of whole rock abundances of P_2O_5 for the syenogranite compared with the monzogranite (Fig. 7i) suggest a process other than fractionation linking the monzogranite and the syenogranite. The abundance of P_2O_5 in the rims of feldspars indicates that there was a delay in the precipitation of apatite in the syenogranite. Such a delay may be due to a higher temperature and/or higher SiO_2 content of the parent magma of the syenogranite (Evans and Hanson 1993; Ayres and Harris 1997). If the former, it implies that the syenogranitic magma was a separate, hotter magma pulse different from the monzogranitic magma, rather than a fractionate of it. A late precipitation of apatite in the syenogranite is also evident in Fig. 15b, where P is homogeneously distributed within the plagioclase crystal, with only a few apatite crystallites present towards the plagioclase crystal rim.

Clarke et al. (1993) suggested that fluid-rock interaction played an important role in the evolution of leucogranite bodies in the SMB. Features in the New Cornwall syenogranite, such as the presence of miarolitic cavities (Fig. 3b), the pegmatitic mineral clots (Fig. 3c), and secondary muscovite indicate the presence of abundant late fluids. On the other hand, geochemical indicators do not suggest a strong influence of fluid. The K/Rb ratios of > 160 indicate control by crystal-melt equilibria, according to Taylor (1965) and Shaw (1968). Likewise, the Ta/Nb ratio shows no evidence of fluid interaction. The presence of oligoclase plagioclase also suggests that interaction with fluids was not of major importance. No textural evidence is seen for alteration by P-rich fluids, of the type recognized by Logothetis (1985), and the F content of the syenogranite is unusually low compared with other SMB rocks. There is, therefore, no evidence that the New Cornwall syenogranite developed by post-magmatic, open system, hydrothermal alteration of the Whale Lake monzogranite, as suggested by Clarke et al. (1993) for the formation of "associated" leucogranite.

The similarities in Nd isotopes, LREE, and some other geochemical indicators (A/CNK, TiO_2, Ba, Rb/K, Nb, Sr, Zr, Nb) between the monzogranite and syenogranite suggest that the two rock types were derived by partial melting from a common source. Both the Whale Lake monzogranite and the New Cornwall syenogranite then evolved independently by fractional crystallization and late fluids played only a minor role in the further evolution of the syenogranite. We conclude that this represents a third mode of development of mineralized leucogranite in the SMB, in addition to the two recognized by Clarke et al. (1993).

CONCLUSIONS

1. The leucocratic New Cornwall syenogranite developed at the southern margin of the Whale Lake monzogranite with a sharp or narrow gradational contact.
2. The syenogranite contains accessory biotite, muscovite, zircon, tourmaline, andalusite, and cordierite. Mineralized miarolitic cavities are common.

3. Binary element plots for some elements show the same regular trend for both monzogranite and syenogranite, but variations in trace elements such as Rb, Ba, Th and LREE suggest that the syenogranite was not derived from the monzogranite by fractional crystallization. Ratios such as A/CNK (~ 1.25), Rb/K (~ 215) and Nb/Ta (~ 3.5) indicate that the syenogranite is not highly fractionated. The syenogranite has similar LREE but lower Eu and HREE compared with monzogranite.
4. Both the New Cornwall syenogranite and the Whale Lake monzogranite have similar Nd isotope compositions, with ε_{Nd} between -1.8 and -2.2, in contrast to the substantial range in ε_{Nd} found elsewhere in the SMB.
5. The syenogranite differs geochemically in many ways from both "associated" and "independent" leucogranite of Clarke et al. (1993). These characteristics, coupled with the observations listed above, suggest that it was not developed either by open-system interaction with fluid, nor by extreme fractionation.
6. The geochemical similarities between the New Cornwall syenogranite and the Whale Lake monzogranite, notably their high A/CNK, low Rb and Nb, and small range of ε_{Nd}, resulted from partial melting of a common source.

ACKNOWLEDGEMENTS

REFERENCES

ABDEL-RAHMAN, A.-F.M. 1994. Nature of biotites from alkaline, calc-alkaline and peraluminous magmas. Journal of Petrology, 35, pp. 525–541.
ALLAN, B.D., & CLARKE, D.B. 1981. Occurrence and origin of garnet in the South Mountain Batholith, Nova Scotia. Canadian Mineralogist, 19, pp. 19–24.
AYRES, M., & HARRIS, N. 1997. REE fractionation and Nd-isotope disequilibrium during crustal anatexis: constraints from Himalayan leucogranites. Chemical Geology, 139, pp. 249–269.
CLARKE, D.B., MACDONALD, M.A., REYNOLDS, P.H., & LONGSTAFFE, F.J. 1993. Leucogranites from the Eastern part of the South Mountain Batholith, Nova Scotia. Journal of Petrology, 34, pp. 653–679.
CLARKE, D.B., HALLIDAY, A.N., & HAMILTON, P.J. 1988. Neodymium and strontium isotopic constraints on the origin of the peraluminous granitoids of the South Mountain Batholith, Nova Scotia, Canada. Chemical Geology, 73, pp. 15–24.
CLARKE, D.B., MCKENZIE, C.B., & MUECKE, G.K. 1976. Magmatic andalusite from the South Mountain Batholith, Nova Scotia. Contributions to Mineralogy and Petrology, 56, pp. 279–287.
DE LA ROCHE, H., LETERRIER, J., GRANCLAUDE, P., & MARCHAL, M. 1980. A classification of volcanic and plutonic rocks using R_1R_2-diagram and major element analyses — its relationships

with current nomenclature. Chemical Geology, 29, pp. 183–210.

EVANS, O.C., & HANSON, G.N. 1993. Accessory-mineral fractionation of rare-earth element (REE) abundances in granitoid rocks. Chemical Geology, 110, pp. 69–93.

FLOYD, P.A., & WINCHESTER, J.A. 1975. Magma type and tectonic setting discrimination using immobile elements. Earth and Planetary Science Letters, 27, pp. 211–218.

HAM, L.J., & KONTAK, D.J. 1988. A textural and chemical study of white mica in the South Mountain Batholith, Nova Scotia: primary versus secondary origin. Maritime Sediments and Atlantic Geology, 24, pp. 111–121.

HENRY, D.J., & GUIDOTTI, C.V. 1985. Tourmaline as a petrogenetic indicator mineral: an example from the staurolite-grade metapelites of NW Maine. American Mineralogist, 70, pp. 1–15.

HORNE, R.J. 1987. Preliminary geological map of New Germany. Nova Scotia Department of Mines and Energy, Open File Map 87-004.

HORNE, R.J. 1992. Geological Map of New Germany. Nova Scotia Department of Natural Resources, Mines and Energy Branches, Map 93-01.

IRVINE, T.N., & BARAGAR, W.R.A. 1971. A guide to the chemical classification of the common volcanic rocks. Canadian Journal of Earth Sciences, 8, pp. 523–548.

LOGOTHETIS, J. 1985. Economic geology of the New Ross - Vaughan Complex. In Guide to the granites and mineral deposits of southwestern Nova Scotia. Edited by A.K. Chatterjee and D.B. Clarke. Nova Scotia Department of Mines and Energy, Paper 85-3, pp. 41–62.

MACDONALD M.A., HORNE, R.J., COREY, M.C., & HAM, L.J. 1992. An overview of recent bedrock mapping and follow-up petrological studies of the South Mountain Batholith, southwestern Nova Scotia, Canada. Atlantic Geology, 28, pp. 7–28.

MILLER, C.F., STODDARD, E.F., BRADFISH, L.J., & DOLLASE, W.A. 1981. Composition of plutonic muscovite: genetic implications. Canadian Mineralogist, 19, pp. 25–34.

PE-PIPER, G., & PIPER, D.J.W. 1989. The upper Hadrynian Jeffers Group, Cobequid Hills, Avalon Zone of Nova Scotia: a back-arc volcanic complex. Geological Society of America Bulletin, 101, pp. 364–376.

PE-PIPER, G., & JANSA, L.F. 1999. Pre-Mesozoic basement rocks offshore Nova Scotia, Canada: New constraints on the accretion history of the Meguma Terrane. Geological Society of America Bulletin, 111, pp. 1773–1791.

SAAVEDRA, J. 1978. Geochemical and petrological characteristics of mineralised granites of the west centre of Spain. In "Metallization associated with acid magmatism." Edited by M. Stemprok, L. Burnol, and G. Tischendorf. Geological Survey of Czechoslovakia, 3, pp. 279–291.

SHAW, D.M. 1968. A review of K-Rb fractionation trends by covariance analysis. Geochimica et Cosmochimica Acta, 32, pp. 573–601.

SMITH, T.E. 1979. The geochemistry and origin of the Devonian granitic rocks of southwest Nova Scotia. Geological Society of America Bulletin, 90, pp. 850–885.

STRECKEISEN, A. 1976. To each plutonic rock its proper name. Earth Science Review, 12, pp. 1–33.

STRECKEISEN, A., & LE MAITRE, R.W. 1979. A chemical approximation to the modal QAPF classification of the igneous rocks. Neues Jahrbuch für Mineralogie Abhandlungen, 136, pp. 169–206.

SUN, S.-S., & McDONOUGH, W.F. 1989. Chemical and isotopic systematics of oceanic basalts: implications for mantle compositions and processes. In "Magmatism in the Ocean Basins". Edited by A. D. Saunders and M. J. Norry. Geological Society Special Publication, 42, pp. 313–345.

TAYLOR, S.R. 1965. The application of trace element data to problems in Petrology. Physics and Chemistry of the Earth, 6, pp. 133–213.

THORNTON, C.P., & TUTTLE, O.F. 1960. Chemistry of igneous rocks, differentiation index. American Journal of Science, 258, pp. 664–684.

WHALEN, J.B. 1980. Geology and geochemistry of the molybdenite showings of the Ackley City batholith, southeast Newfoundland. Canadian Journal of Earth Sciences, 17, pp. 1246–1258.

Editorial responsibility: Sandra M. Barr